5-2004

Adaptive optimal control design for stable vibration attenuation of active constrained layer damping beam structure

Tatyana G. Korotkova-Egan
University of Texas-Pan American

ADAPTIVE OPTIMAL CONTROL DESIGN
FOR
STABLE VIBRATION ATTENUATION
OF
ACTIVE CONSTRAINED LAYER DAMPING
BEAM STRUCTURE

A Thesis

by

TATYANA G. KOROTKOVA-EGAN

Submitted to the Graduate School of the
University of Texas Pan American
In partial fulfillment of the requirements for the degree of

MASTER OF SCIENCE

MAY 2004

Major subject: Mechanical Engineering

ADAPTIVE OPTIMAL CONTROL DESIGN
FOR
STABLE VIBRATION ATTENUATION
OF
ACTIVE CONSTRAINED LAYER DAMPING
BEAM STRUCTURE

A Thesis
by
TATYANA G. KOROTKOVA-EGAN

Approved as to style and content by:

Dr. Javier A. Kypuros PhD., Chair
Assistant Professor, University of Texas Pan American

Dr. Hashim S. Mahdi PhD.
Chair of the Mechanical Engineering Department
University of Texas Pan American

Subhash Bose

Dr. Subhash C. Bose PhD.
Chair of the Manufacturing Engineering Department
University of Texas Pan American

Dr. Arturo A. Fuentes PhD.
Assistant Professor, University of Texas Pan American

May 2004

ABSTRACT

Korotkova-Egan, Tatyana, Adaptive Optimal Control Design for Stable Vibration Attenuation of Active Constrained Layer Damping Beam Structure. Master of Science (MS), May 2004, 74 pp., 14 figures, 2 tables, references, 45 titles.

Vibration suppression using active constrained layer damping (ACLD) has proven to be an invaluable means for improving the performance of a wide variety of engineering systems. The ACLD creates the hybrid of active and passive damping, attaining favorably high damping characteristics, while at the same time, combines unattractive attributes of both treatments, such as stability sensitivity. Control efforts are needed to achieve an adequate performance of the structures treated with ACLD.

The purpose of this research is to investigate theoretically and numerically the adaptive optimal controller of the constrained layer damped beam system, using the classical three-layered distributed-parameter model that utilizes Hamilton's principle in the derivation. Particular emphasis is placed on controlling and stability analysis of the first bending mode of the response on the harmonic excitation using proportional control law. A new technique for prediction of optimal damping performance for fully treated beam/ACLD system using time-domain analysis of control is proposed. Comparison between analytical and numerical results, as well with experimental results found in the literature, showed that the proposed strategy is very simple and efficient in constructing the adaptive optimal control gains for amplitude attenuation of structural vibrations.

DEDICATION

This thesis is dedicated

to my father

Gennadiy S. Korotkov,

who established my human conception of the world,

and

to my husband

Allen M. Egan,

who has given me invaluable educational opportunities and support.

"… It is for the happiness of those united in society to harmonize as much as possible in matters which they must of necessity transact together…"

T.Jefferson,

the third President of Unites States.

ACKNOWLEDGEMENTS

This work is partially funded by the NASA grant to the University of Texas Pan American. The author gratefully acknowledges the Mechanical Engineering Department Staff & Faculty. Special thanks are due to Dr.J.A.Kypuros Dr. H.S.Mahdi, Dr. S.C.Bose, Dr. A.A.Fuentes, for their constructive comments.

TABLE OF CONTENTS

APPENDIXES

LIST OF FIGURES

LIST OF TABLES

CHAPTER 1

INTRODUCTION

Vibration, the repetitive motion of objects relative to a stationary frame of reference or nominal position, occurs in most machines, structures and dynamic systems. Vibration is normally viewed as undesirable, not only owing to the resulting unpleasant motions, noise, and dynamic stresses possibly leading to fatigue and failure of the structure or machine, but also to energy losses and degraded performance. Increasing the capability and life of equipment often requires reducing the mechanical vibration of a system. Technological advances have further enhanced the means of controlling vibration in mechanical engineering, aerospace engineering, civil engineering and related applications.

To reduce vibration response and avoid structural instability conventional passive damping treatments [2,13-14,28-29] have been applied to machines and structures widely over the previous century. The simplest form of passive damping treatment is the free layer damper shown in Figure 1(a), which is a viscoelastic material (VEM) bonded to the base structure. Vibration of the base structure strains the viscoelastic material, and the associated strain energy is converted into heat. Dissipation of the heat from the structure reduces its vibration energy. Another form of passive constrained damping treatment (PCLD) is shown in Figure 1(b), where a constraining layer is attached to the viscoelastic layer to increase its strain and enhance its damping characteristics [1,3,4,36,39,44].

Although these damping treatments can provide high damping ratios and reliable performance, a considerable weight is added to the vibrating structure. Moreover, once the passive damping is installed, it cannot be adjusted and cannot adapt to changeable environments. This poses a serious limitation to their practical use in applications.

Such problems can be avoided through the use of active damping treatments. In the simplest form, two piezoelectric layers (PZM) are bonded symmetrically to a structure such that bending can be induced by expanding one layer and contracting the other. As with passive damping, the optimal configuration and distribution of the piezoelectric layers are essential to achieving high performance characteristics. Rao and Sunar [33], Baz and Park [9-10,31-32,36] outlined the considerable interest in the area of active vibration control. However, serious concerns have been raised. For example damping can be obtained only by control efforts, function of active components and control hardware can cause the structure to lose its active damping completely and result in instability.

Recently, considerable interest has been directed on controlling the vibration of structures with the active constrained layer damping (ACLD) treatment [5-8,11-12,19,21,24-27,34-35,37,41-42,45]. The ACLD treatment generally consists of a piece of viscoelastic damping material sandwiched between an active piezoelectric layer and a host structure (Figure 1(c)). It has been recognized, the active piezoelectric action in an ACLD configuration will enhance the viscoelastic layer ability by increasing its shear angle during operation. Control of high-frequency vibrations can be easily attained with the passive damping, and control of low-frequency vibrations becomes possible with the active component. The treatment requires less control effort than pure active damping.

ACLD systems have been studied by various researchers. They are the elastic-elastic

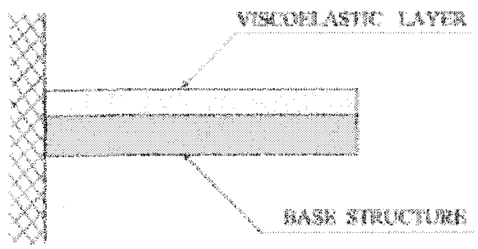

a) Passive (unconstrained)

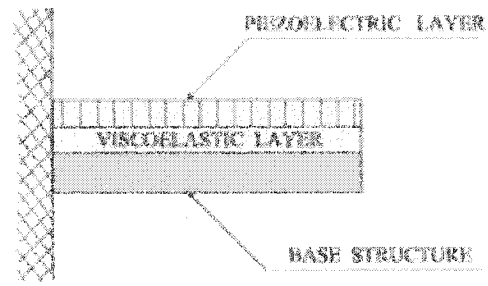

b) Passive (constrained)

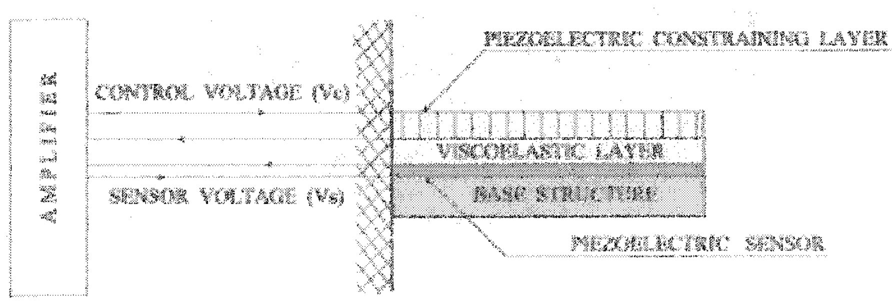

c) Active (constrained)

Figure 1. Passive and Active Layer Damping.

two-layer beam (Timoshenko, 1925; Hess 1969), elastic-VEM two-layer beam (Oberst, 1952), elastic-VEM-elastic tree- layer PCLD beam (Kervin, 1959; DiTaranto, 1965; Mead and Markus, 1969; Yan and Dowell, 1972), elastic-PZM two layer beams (Crawley and de Luis, 1987), and the elastic-VEM-PZM tree layer ACLD beams (Baz, 1993; Leibowitz and Vison, 1993; McTavish and Hughes, 1993; Shen, 1994; Wereley,1995; Baz, 1997; Austin and Ingman, 1998). A number of authors have considered finite element method to predict the performance of constrained layer damped simple structures such as beams, plates and shells (Liu and Wang, 1998; Chen and Levy, 1998; Agafa and Baz, 1999; Batra, 2000; Baz and Chen, 2000; Park and Baz, 2001; Balamurugan and Narayanan, 2002;Sun and Tong, 2002; Wang, 2003).

In the present study, the emphasis is placed on extending the model of A.Baz [9-11, 31, 32, and 34-37]. Equations of motion, introduced in works of A.Baz, are accepted as a basis for the developed in this study analysis, contained in determination of the optimal damping performance of the beam-type structure fully treated with ACLD undergoing the typical situation of transverse harmonic excitation. The solution of distributed parameter differential equations of motion is derived in time-response analysis of control. The thesis is organized in nine chapters. In chapter 1 the brief introduction is given. The problem statement and research objective is outlined in chapter 2, and chapter 3 describes the experimental setup for testing of damping performance. The variational model of ACLD is developed in chapter 4 and numerical solutions of the model are presented in chapter 5. In chapter 6 and 7 controllability and stability issues are considered. In chapter 8 the adapted optimal controller is devised. Chapter 9 gives a summary of results and conclusions.

CHAPTER 2

PROBLEM STATEMENT AND RESEARCH OBJECTIVE

Although the effectiveness of the ACLD systems has been demonstrated and some analyses have been performed to understand its characteristics, a comprehensive and generic study of controllability and stability boundary has not been completed. At the same time, these aspects are an important issue used in design of nonlinear and optimal feedback control of the system treated with ACLD.

There are two important approaches to the design of feedback controllers for nonlinear systems: Lyapunov stability methods and optimal control theory. On the surface, these two approaches might not appear to have much in common. Lyapunov stability does not address optimality, while optimal control theory generally provides only open-loop control, which need not provide stability. However, when function optimizing feedback controller is combined with Lyapunov stability method, the resulting controller do contain global information. These function optimizing Lyapunov controllers have proven to be highly effective and also robust with respect to uncertainties in system models, noisy inputs, and so on.

The goal of this paper is to conduct the above issues to design an optimal controller of the beam/ACLD system in order to reduce displacement amplitudes while maintaining the stability of the structure. The design of the controller is based on the integrated approach on fundamental topics of stability, controllability, and optimality, and on the corresponding geometry associated with these topics.

CHAPTER 3

EXPERIMENTAL SET-UP AND PROCEDURES

Figure 2 shows a photograph of the experimental set-up used in testing the effectiveness of the Active Constrained Layer Damping in attenuating the vibration of the test beam compared to conventional passive layer damping. The beam/ACLD system is mounted in a cantilevered configuration in vibration exciter (Model 480, Bruel & Kjaer, Denmark). Fixed over the base beam uniformly distributed piezoelectric foil (PTS-1195, Piezo-electric Products, NJ) treated with an acrylic viscoelastic film (2552-3M-TM) is used to control bending vibrations of the system.

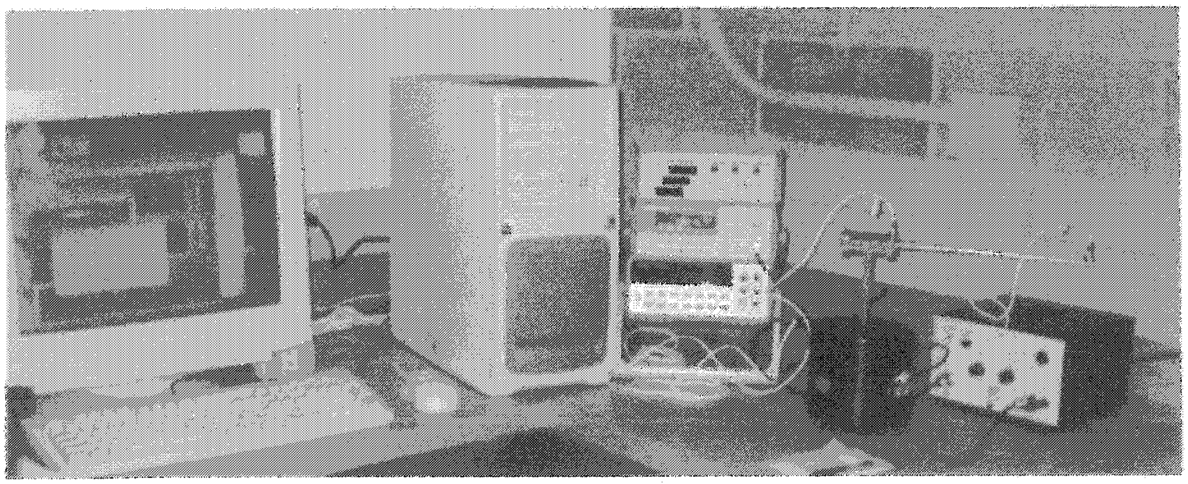

Figure 2. Experimental set-up for beam/ACLD system.

Figure 3 shows a schematic drawing of the set-up indicating that the internal function generator (Model WH2270, Bruel & Kjaer, Denmark) is used to generate a sine-wave sweep. This sine wave is used to excite the beam/ACLD system through a power amplifier (Model 2706 Bruel & Kjaer, Denmark). Displacement signal is measured by a sensor (Model 3061-120, ENDEVCO, California) at the end of the test beam and fed to the computer-analyzer to determine the acceleration and then, after double integration, displacement content. The input wave and the system response are automatically displayed and stored in the analyzer. Figure 3 also shows that another amplifier combined with voltage piezo-actuator (Model E-663 LVPZT, Wilcoxon Research, MD) is independently used to obtain the constraining signal between the piezo-actuator and piezo-sensor. The resulting control voltage is sent via the amplifier to the piezoelectric actuator layer and the computer-analyzer to determine the amplitude of vibration.

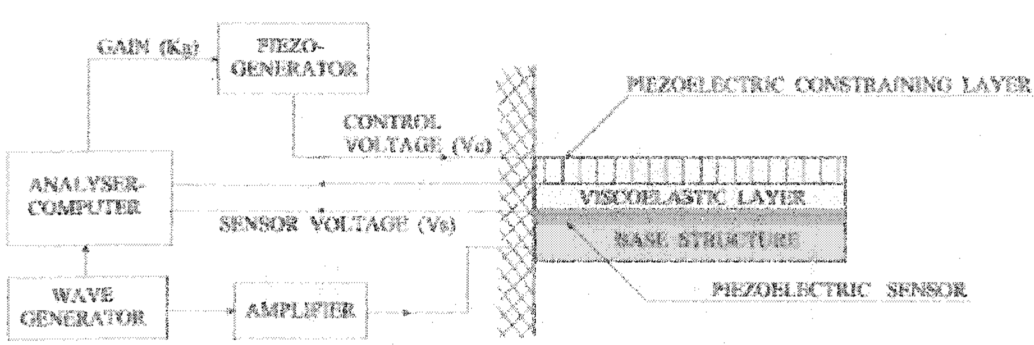

Figure 3. Schematic drawing of the experimental set-up.

CHAPTER 4

4. VARIATIONAL MODELING

4.1. SYSTEM DESCRIPTION

The schematic representation of three-layer composite ACLD treatment bonded to the base structure is illustrated in Figures 1(c) and 3. The viscoelastic damping layer is placed between two piezoelectric layers, active constraining on the top and piezoelectric sensor on the bottom. The sensing, as indicated by the sensor voltage V_s, is provided by the piezoelectric layer which is directly bonded to the beam surface. The actuation is generated by the other piezoelectric layer which acts as an active constraining layer that is activated by the control voltage V_c. With appropriate strain control through proper manipulation of V_c, the structural vibration can be damped.

4.2. ASSUMPTIONS OF THE BASIC MODEL

The model has been developed for the system based on the following assumptions:

1) The thickness of the piezo-constraining and viscoelastic layers are very small compared to that of the base structure. Hence the shear deformations in the piezoelectric layer and in the base beam are negligible.
2) The longitudinal stresses in the viscoelastic core are negligible.
3) The transverse displacements $w(x,t)$ of all points on any cross section of the beam with ACLD treatment is assumed to be the same for all layers.

4) The piezoelectric layer and the base beam are assumed to be elastic and dissipate no energy whereas the core is assumed to be linearly viscoelastic. Accordingly, the linear theories of elasticity, viscoelasticity , and piezoelectricity are used.
5) Young's modulus of the viscoelastic material is negligible compared to those of the elastic and piezoelectric layers.
6) There is a perfect continuity at the interfaces, and no slip occurs between the layers. In addition, the piezoelectric sensor and the base beam are considered to be perfectly bonded together such that they can be reduced to a single equivalent layer. Therefore, the original four-layers sandwiched beam reduces to an equivalent three-layers beam.
7) The density and thickness are uniform over the beam.

4.3. GEOMETRY AND KINEMATICS

Figure 4 shows the drawing of the transverse cross-section of the proposed three-layers cantilever beam treated with ACLD. The piezoelectric cover sheet is connected to an external voltage source as the control input.

The shear strain γ in the core is:

$$\gamma(x,t) = \left[hw_x(x,t) + u_1(x,t) - u_3(x,t)\right] / h_2 \tag{1}$$

where,

$$h = h_2 + (h_1/2) + (h_3/2), \tag{2}$$

$u_1 = u_1(x,t)$ is the longitudinal deflections of the piezo-actuator layer, $u_3 = u_3(x,t)$ is the longitudinal deflection of the beam/sensor layers; $w = w(x,t)$ denotes the transverse deflection of the beam system; subscript x denotes partial differentiation with respect to x; and h_1, h_2, and h_3 define the thicknesses of the piezo-actuator, the viscoelastic layer, the piezo-sensor/base beam system respectively.

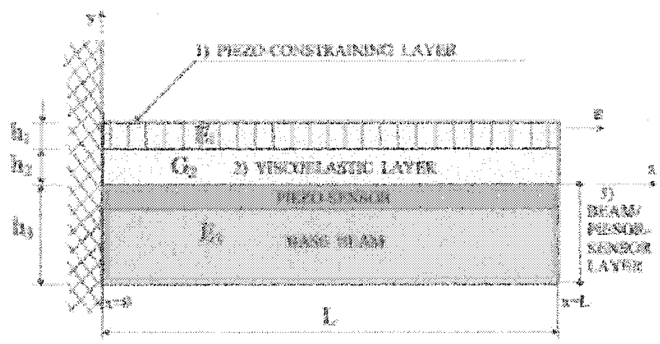

a) undeflected

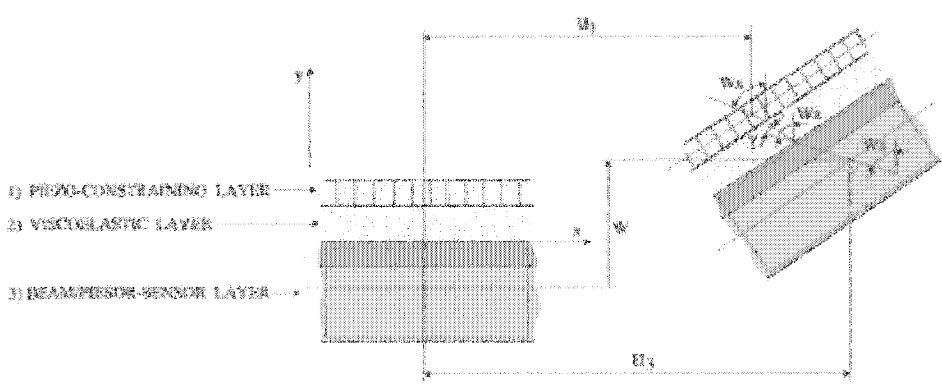

b) deflected

Figure 4. The geometry of the system.

4.4 THE MODEL AND MAIN PARAMETERS

The equations and boundary conditions governing the operation of the beam/ACLD system are obtained by applying Hamilton's principle (A.Baz [9], L.Meirovitch [29]):

$$\int_{t_1}^{t_2} \delta\left(T - \sum_{i=1}^{3} U_i\right) dt + \int_{t_1}^{t_2} \delta\left(\sum_{j=1}^{3} W_j\right) dt = 0, \tag{3}$$

where $\delta(.)$ denotes the first variation in the quantity inside the parentheses.

The kinetic energy T associated with the transverse deflection $w(x,t)$ is given by:

$$T = \frac{1}{2} mb \int_0^L w_t^{\,2} dx \ . \tag{4}$$

The potential energy associated with the extension is:

$$U_1 = \frac{1}{2} K_1 b \int_0^L u_{1x}^{\ \ 2} dx + \frac{1}{2} K_3 b \int_0^L u_{3x}^{\ \ 2} dx \ . \tag{5}$$

The potential energy associated with bending is:

$$U_2 = \frac{1}{2} Db \int_0^L w_{xx}^{\ \ 2} dx \ . \tag{6}$$

The potential energy of shearing is:

$$U_3 = \frac{1}{2} G_2' h_2 b \int_0^L \gamma^2 dx \ . \tag{7}$$

The work W_1 done by the external transverse loads q acting on the beam/ACLD system is given by:

$$W_1 = b \int_0^L qw \ dx \ . \tag{8}$$

The work done by the piezoelectric control forces is given by:

$$W_2 = K_1 \int_0^L \varepsilon u_{1x} \ dx \ . \tag{9}$$

The work W_3 dissipated in the viscoelastic core is given by:

$$W_3 = -hb \int_0^L \tau\gamma \, dx . \tag{10}$$

In the equations above m is the mass per unit width and unit length of the beam/ACLD system, L is the beam length and b is the beam width. $K_1 = E_1 h_1$ and $K_3 = E_3 h_3$ with E_1 and E_3 denoting Young's modulus of the piezo-actuator layer and beam/sensor system. $D = (E_1 I_1 + E_3 I_3)/b$ with $E_1 I_1$ and $E_3 I_3$ denoting the flexural rigidity of piezo-actuator and the beam/sensor layer, respectively. The storage shear modulus of the viscoelastic layer is G_2' and ε is the strain induced in the piezoelectric constraining layer. In the equation (10), τ is the dissipative shear stress developed by viscoelastic core, given by:

$$\tau = (G_2' \eta / \omega)\gamma_t = (G_2' \eta)\gamma i \tag{11}$$

where, η denotes the loss factor of the viscoelastic core, $\omega = (n\pi/L)^2 \sqrt{(E_1 I_1 + E_3 I_3)/m}$ is the angular natural frequency of the n mode of the structure [16, 17]; $i = \sqrt{-1} = \dfrac{\gamma_t}{\omega\gamma}$.

The resulting equations of the beam/ACLD system are:

$$-K_1 u_{1xx} + G_2 / h_2 (u_1 - u_3 + hw_x) = 0 , \tag{12}$$

$$-K_3 u_{3xx} - G_2 / h_2 (u_1 - u_3 + hw_x) = 0 , \tag{13}$$

$$Dw_{xxxx} + mw_{tt} - G_2 h / h_2 (u_{1x} - u_{3x} + hw_{xx}) - q = 0 , \tag{14}$$

where,

$$G_2 = G_2'(1 + \eta i) = G_2'\left(1 + \frac{\eta \gamma_t}{\omega\gamma}\right) \tag{15}$$

is the complex modulus of the viscoelastic material.

For a cantilevered beam, the above equations are subject to the following boundary conditions:

$$\text{at } x=0: \quad u_1=0, \quad u_3=0, \quad w=0, \quad w_x=0; \tag{16}$$

$$\text{at } x=L: \quad u_{1x}=\varepsilon, \quad u_{3x}=0, \quad w_{xx}=0, \quad Dw_{xxx}-G_2h/h_2(u_1-u_3+hw_x)=0. \tag{17}$$

Therefore, the particular nature of operation of the beam/ACLD system implies the existence of boundary control action ε.

CHAPTER 5

5. SOLUTION OF EQUATIONS OF MOTION

5.1. OVERVIEW

The governing equations of the beam/ACLD structure (12)-(14) are the system of partial differential equations of fourth order with respect to the spatial variable x and second order with respect to the time variable t, whereas the space and time variables are mutually independent. Specifically, at any given moment t, the system vibrates in a fixed shape function, and therefore at all times, the structure will maintain a particular mode shape. Also, at a given point x of the structure, the value of the shape function will be fixed, the structure will vibrate according to the time response. Hence, the time and space functions are separable for a modal motion (C.W.Silva [40]).

With this qualitative understanding, the modal analysis for a separable solution of the form:

$$u_1(x,t)=\hat{u}_1(x)\tilde{u}_1(t);\quad u_3(x,t)=\hat{u}_3(x)\tilde{u}_3(t);\quad w(x,t)=\hat{w}(x)\tilde{w}(t);\quad \gamma(x,t)=\hat{\gamma}(x)\tilde{\gamma}(t); \tag{18}$$

is applicable.

5.2. DEVELOPMENTAL MODEL FOR APPLICATIONS

Substituting equations (1) and (15) in equations of motion (12)-(14) gives the following system:

$$-K_1 u_{1xx} + G_2'\left(\gamma + \frac{\eta}{\omega}\gamma_t\right) = 0, \tag{19}$$

$$K_1 u_{1xx} + K_3 u_{3xx} = 0, \tag{20}$$

$$Dw_{xxxx} + mw_{tt} - G_2' h\left(\gamma_x + \frac{\eta\gamma_t\gamma_x}{\omega\gamma}\right) - q = 0, \tag{21}$$

$$\gamma = \left[hw_x + u_1 - u_3\right]/h_2. \tag{22}$$

From equation (20) :

$$u_{3x} = -\frac{K_1}{K_3}u_{1x} + C_1,$$

where C_1 is the constant of integration.

At $x = L$, using $u_{1x} = \varepsilon$, $u_{3x} = 0$ from boundary conditions (17), $C_1 = \varepsilon$, that results in:

$$u_{3x} = -\frac{K_1}{K_3}u_{1x} + \varepsilon.$$

Differentiating the equation of boundary condition (17) with respect to x gives:

at $x = L$ $$w_{xxxx} = G_2 h\varepsilon / h_2\ , \tag{23}$$

wher, from equation (15):

$$G_2 = G_2'\left(1 + \frac{\eta\gamma_t(x,t)}{\omega\gamma(x,t)}\right) = G_2'\left(1 + \frac{\eta\hat{\gamma}(x)\tilde{\gamma}_t(t)}{\omega\hat{\gamma}(x)\tilde{\gamma}(t)}\right) = G_2'\left(1 + \frac{\eta\hat{\gamma}_t(t)}{\omega\hat{\gamma}(t)}\right),$$

that implies the independence of the modulus G_2 from the spatial coordinate x.

Incorporating the boundary condition (23) with the equation of motion (14) at $x = L$ yields the following equation:

$$w_{tt}(L,t) = q(L,t). \tag{24}$$

Considering separable functions of the form (18), equation (24) indicates:

$$\hat{w}_{tt}(t) = \frac{\hat{q}(L)\tilde{q}(t)}{m\hat{w}(L)}\ . \tag{25}$$

Therefore, the resulting rearranged equations of motion of the beam/ACLD system are:

$$-K_1 u_{1xx} + G_2'\left(\gamma + \frac{\eta}{\omega}\gamma_t\right) = 0, \tag{26}$$

$$u_{3x} = -\frac{K_1}{K_3}u_{1x} + \varepsilon, \tag{27}$$

$$D\hat{w}_{xxxx}(x)\tilde{w}(t) + m\hat{w}(x)\tilde{w}_{tt}(t) - G_2'h\left(\gamma_x + \frac{\eta\gamma_t\gamma_x}{\omega\gamma}\right) - q = 0, \tag{28}$$

$$\gamma = \left[h\hat{w}_x(x)\tilde{w}(t) + u_1 - u_3\right]/h_2, \tag{29}$$

with the time function $\hat{w}(t)$ defined by the equation (25), and where previous set of eight boundary conditions (16), (17) is reduced to the following six equations:

$$\text{at } x = 0: \qquad u_1 - u_3 = 0, \qquad w = 0, \qquad w_x = 0; \tag{30}$$

$$\text{at } x = L: \qquad u_{1x} - u_{3x} = \varepsilon, \qquad w_{xx} = 0, \qquad Dw_{xxx} - G_2'h/h_2\left(\gamma + \frac{\eta\gamma_t}{\omega}\right) = 0. \tag{31}$$

The present model equations (1), (12)-(14) and (16), (17) are manipulated differently to obtain the modified representation of the ACLD/system which is then used to develop the numerical solution of the functions (18), as shown in section 3.3.

5.3. NUMERICAL EVALUATIONS

5.3.1. *The Program and Materials*

The performance of the cantilever beam structure treated with ACLD patch corresponding to the first mode is evaluated by numerical simulation of model equations (26)-(31) with MATLAB/SIMULINK software (Appendix A, B). The general algorithm of simulation is shown in Figure 3.

It is important to note the advantage of the developed modified model contained in the fact that the separable representation of the functions u_1 and u_3 is unnecessary and became superfluous because of the presence of only spatial differentials of those functions. In different of ones, the function of transverse deflection w maintains both time and spatial differentiations and, therefore, the analysis with a separable solution preferred given by

$$w(x,t) = \hat{w}(x)\widetilde{w}(t) .$$

The second aspect is the use of SIMULINK block procedures working with respect to spatial continuous x variable instead of conventional way of time continuous simulation. Such permutation is allowed by mutual independency of x and t variables for a modal motion, as it has been mentioned above, and by their continuity in physical space.

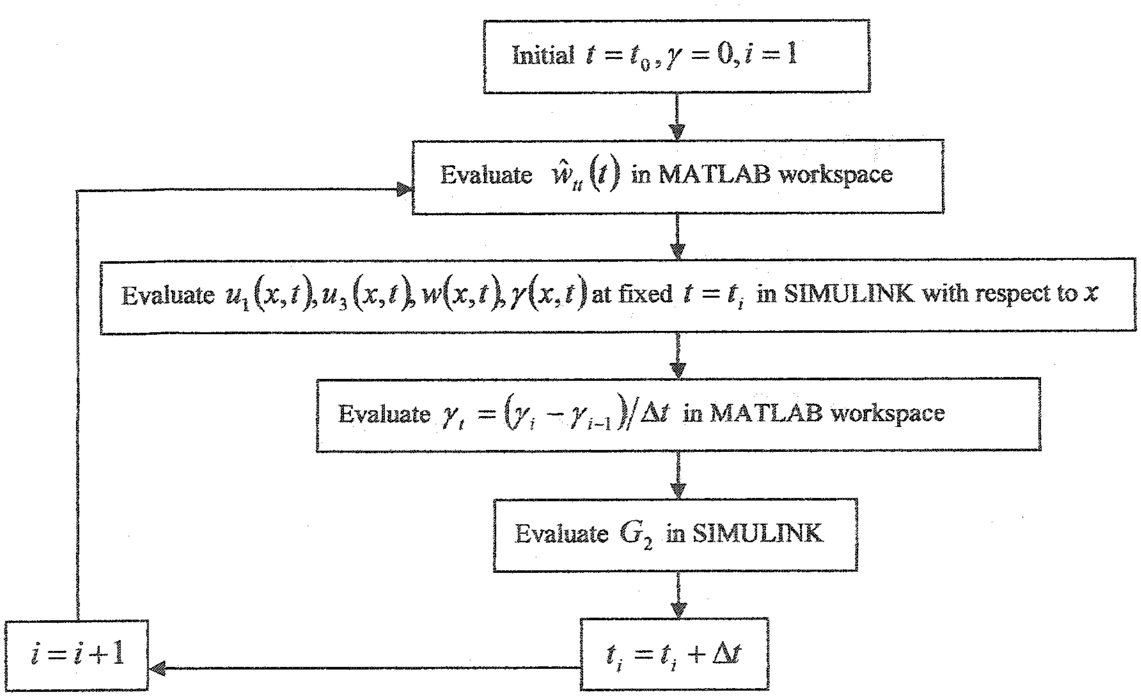

Figure 5. Algorithm of the numerical solution.

The time derivative of the shear strain function $\gamma_t(x,t)$ is accounted as a time variation $\delta\gamma/\partial t$ of values of γ function between neighboring time moments of simulation at each step of time.

The strain ε induced in the piezoelectric constraining layer is implemented in terms of displacement feedback given by:

$$\varepsilon = -K_g \max[w(x,t)], \tag{32}$$

where, K_g is the gain of the boundary controller and $w(L,t)$ is the maximum transverse displacement at free end of the beam/sensor.

The methods outlined here are demonstrated on the cantilevered steel beam in Figure 4, whose parameters are given in Table 1. The beam is treated with an acrylic base viscoelastic material, followed by a piezoelectric constraining film. The beam structure is subject to sinusoidal transverse load q acting at its free end.

TABLE 1.

System parameters

Piezoelectric layer:	$h_1 = 0.625(mm)$	$E_1 = 63(MN/m^2)$	
Viscoelastic layer:	$h_2 = 0.25(mm)$	$\eta = 1.5$	$G_2' = 0.35(MN/m^2)$
Beam/sensor layer:	$h_3 = 1.25(mm)$	$\rho_{steel} = 8(g/cm^3)$	$E_3 = 206.85(MN/m^2)$
External transverse load:	$q = \sin(\omega_d t)(MN)$	$\omega_d = 100(\sec^{-1})$	$f_d = 15.916(Hz)$
Parameters of the system:	$L = 0.1(m)$	$b = 0.025(m)$	$\omega = 2515.6(\sec^{-1})$

5.3.2. *Illustrative Examples*

Presented in Appendixes A, B program and block diagram simulating the model (26)-(31) generate the dynamic illustration of shape functions $u_1(x,t), u_3(x,t)$, $w(x,t)$ and

$\gamma(x,t)$. In this paper the animated graphics is displayed at fixed time moments of maximum altitudinal deflection of shape function w.

Figure 6 provides a few examples of resulting first mode shapes for different values of piezoelectric strain ε and corresponding gain constants K_g: a) $\varepsilon = 0$, $K_g = 0$ (no control); b) $\varepsilon = -0.0188$, $K_g = 5$; c) $\varepsilon = -0.0303$, $K_g = 10$; d) $\varepsilon = -0.0422$, $K_g = 16$ (critical value); e) $\varepsilon = -1.2710$, $K_g = 16.7$. The dependence of the maximum transverse displacement w on controlling constraint ε and corresponding gain values is shown in Table 2 which is also illustrated in Figure 7.

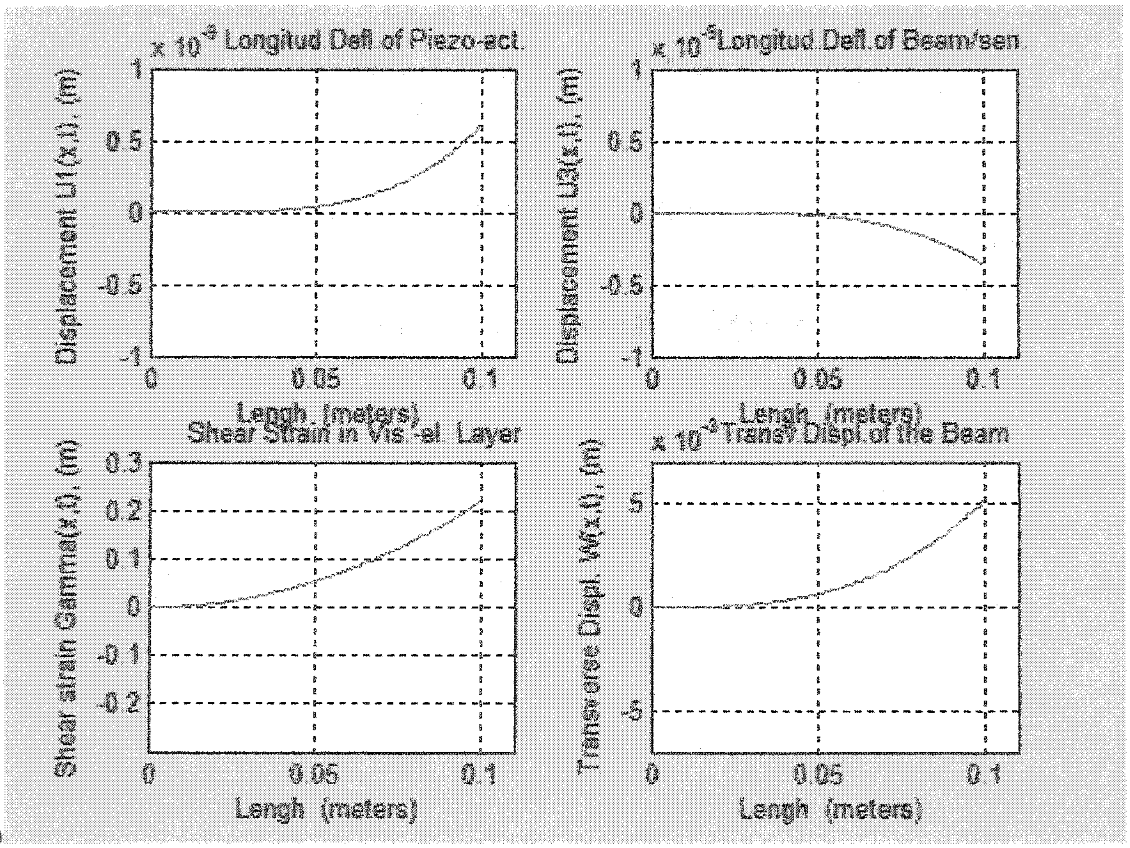

a)

Figure 6. Shape functions at constrained vibrations of the beam/ACLD system:
a) $\varepsilon = 0$, $K_g = 0$ (no control action).

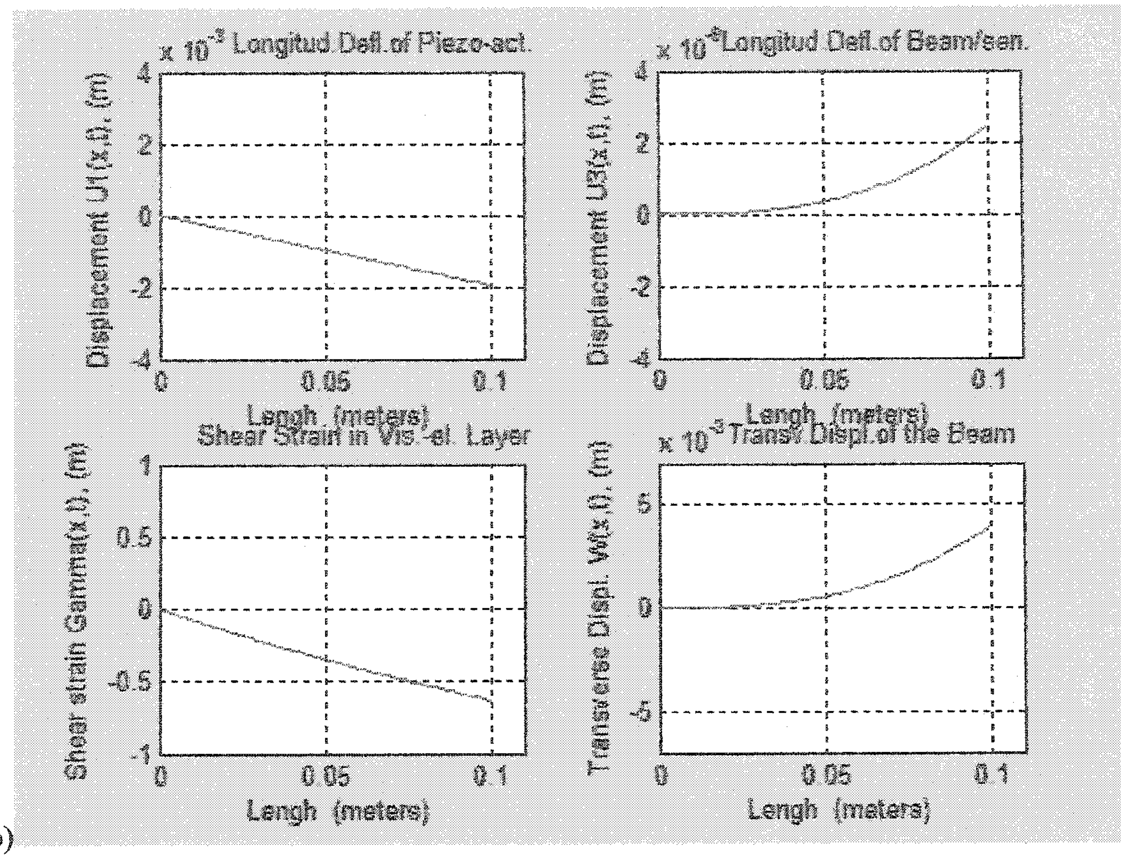

b)

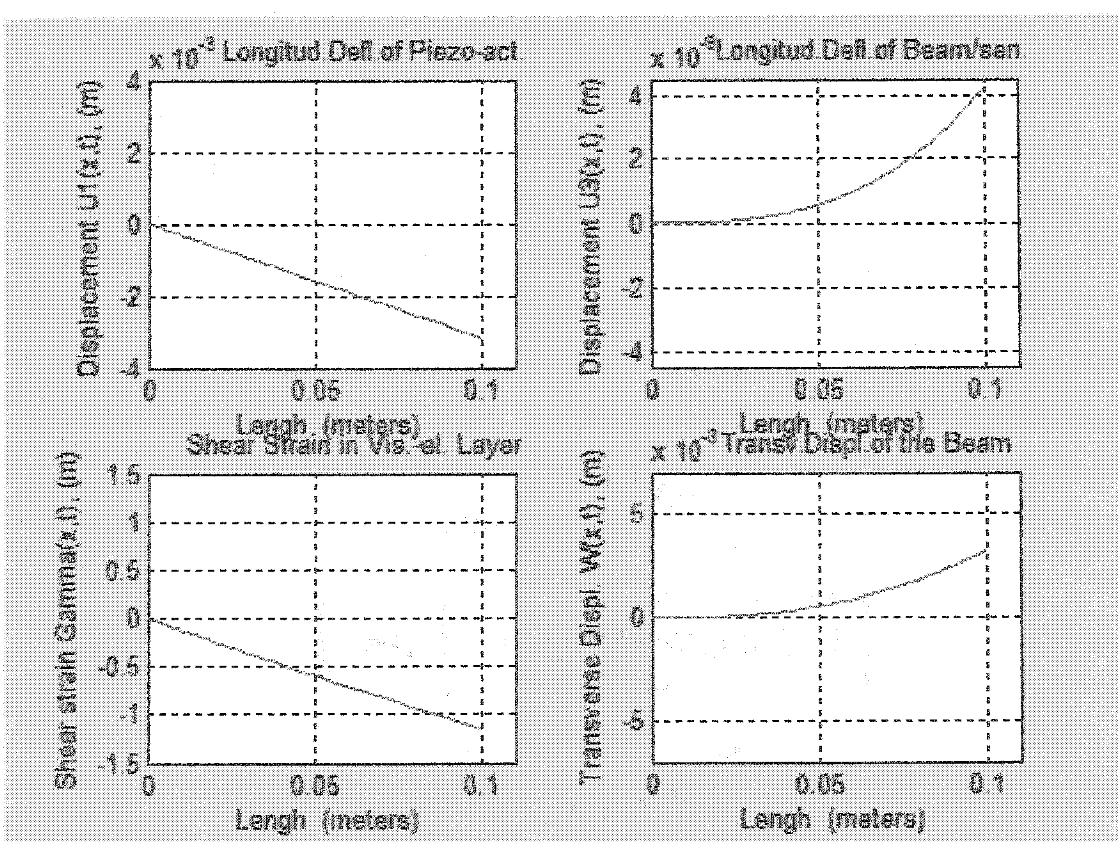

c)

Figure 6. Shape functions at constrained vibrations of the beam/ACLD system:
b) $\varepsilon = -0.0188$, $K_g = 5$; c) $\varepsilon = -0.0303$, $K_g = 10$.

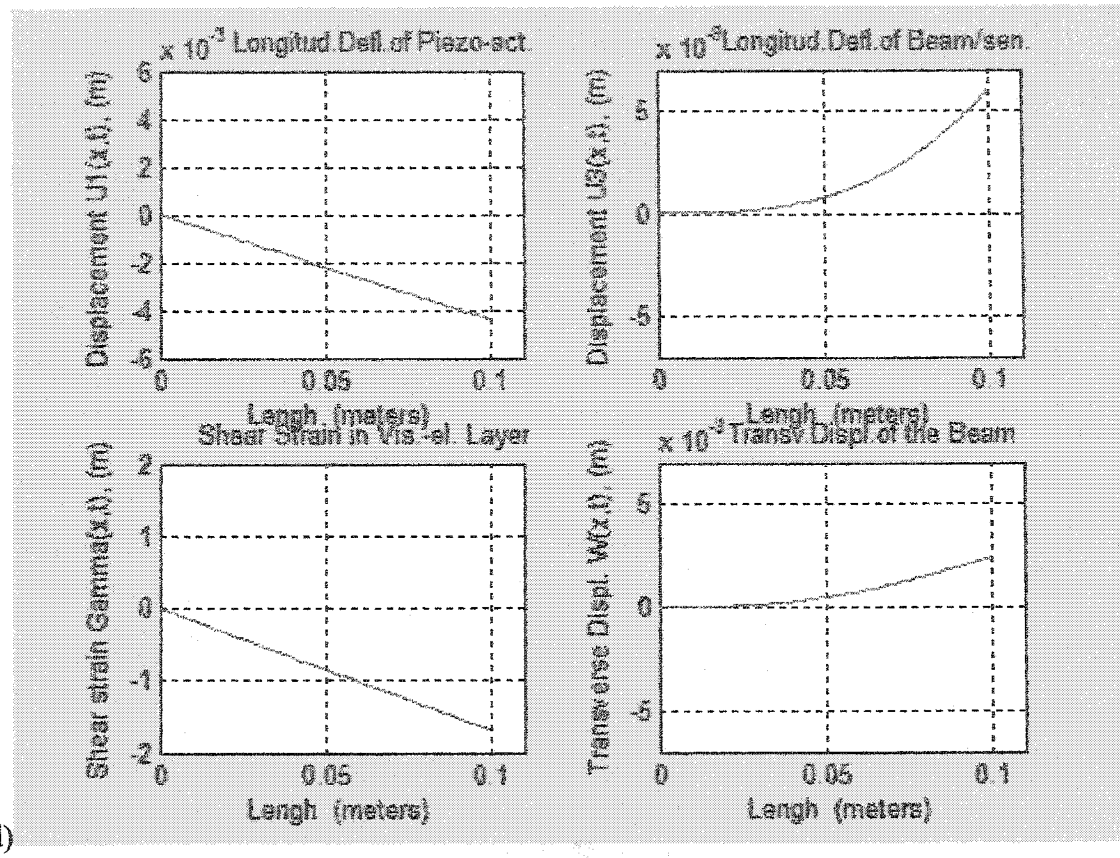

d)

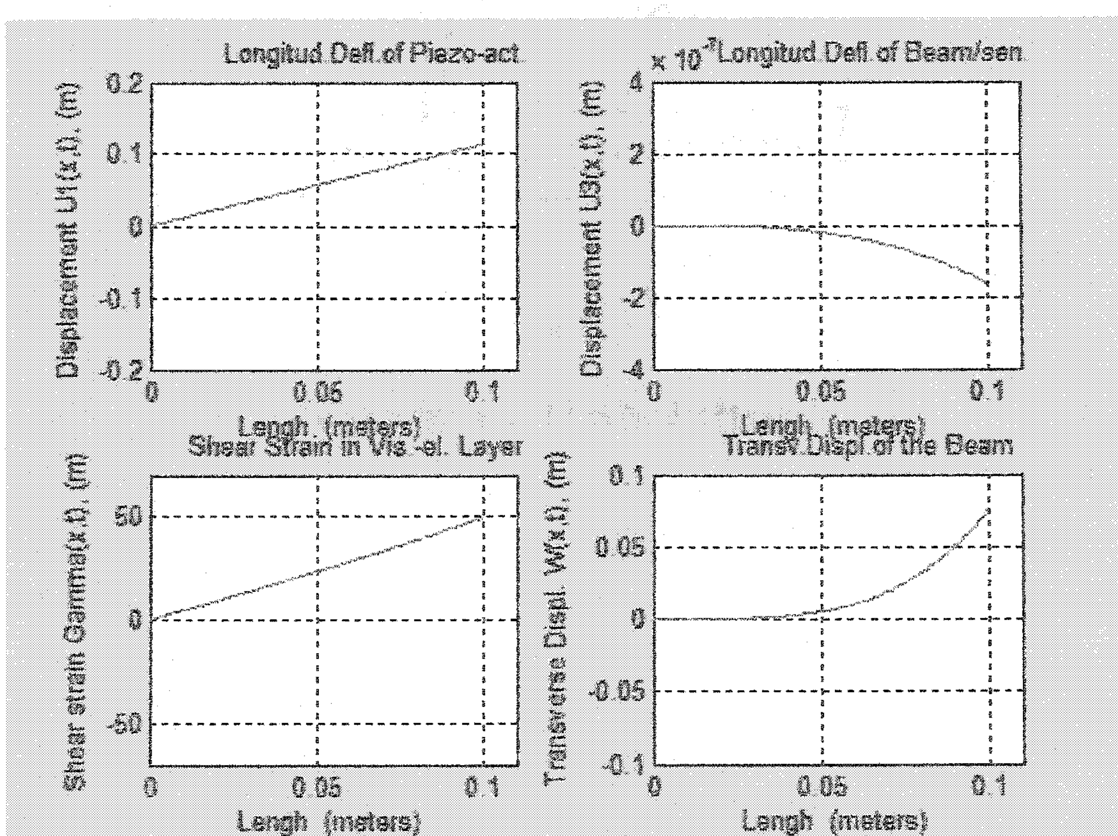

e)

Figure 6. Shape functions at constrained vibrations of the beam/ACLD system: d) $\varepsilon = -0.0422$, $K_g = 16$ (critical value); e) $\varepsilon = -1.2710$, $K_g = 16.7$

TABLE 2.

Maximum transverse displacements at changing piezoelectric strain ε and control gain K_g

K_g	ε	$\max(w)$
0.0	0.0000	0.0050
2.5	−0.0107	0.0043
5.0	−0.0188	0.0038
7.5	−0.0252	0.0034
10.0	−0.0303	0.0030
12.5	−0.0345	0.0028
15.0	−0.0381	0.0025
16.0	−0.0422	0.0026
16.1	−0.0477	0.0030
16.2	−0.0526	0.0032
16.3	−0.0629	0.0039
16.4	−0.065	0.0040
16.5	−0.0666	0.0040
16.6	−0.0678	0.0041
16.65	−0.2909	0.0175
16.7	−1.2710	0.0761
16.8	−10.3841	0.6181

It is evident the maximum transverse deflection w decreases with increasing gain of the boundary controller K_g to a minimum (at $K_g \approx 16$ in this example of simulation) and then increases dramatically, when the operating gain prevails a particular value. Furthermore, operating with different values of parameters and material properties of the structure, the clear positions of a minimum altitudinal deflection and critical value of gain constant were established. Results indicated that amplitude attenuation of about 52% for the first vibration mode was achieved conditional upon control action not exceeding the transitional points.

Such pronounced changes in damping quality produced by the ACLD treatment introduce the utility of the devised optimal controller for the structure.

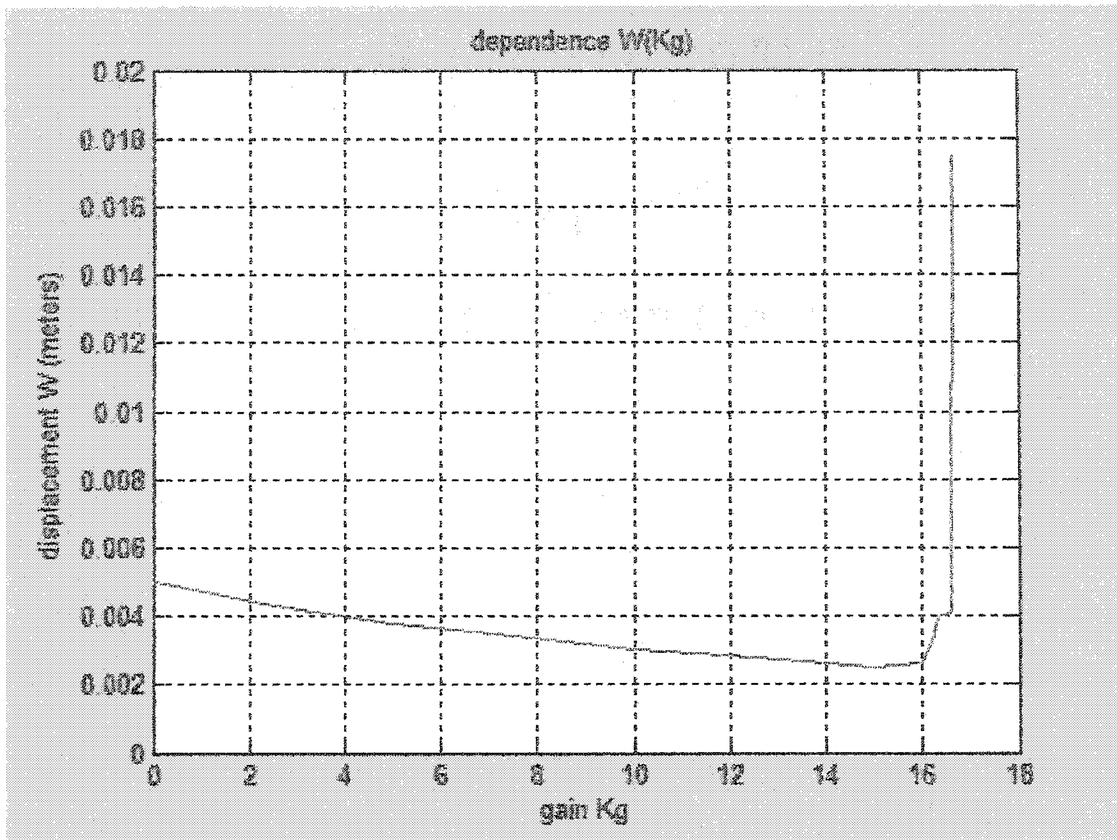

Figure 7. Effect of constraining gain constant on the maximum transverse displacement.

5.3.3. *Energies*

Figure 8 depicts the energies given by (4)-(10) and determined at the moment when the maximum altitudinal deflection is achieved. Those contained herein are plotted by program and block diagram (Attachment C,D) creating the animated motion. The eighth picture of Figure 8 is expressed by Hamilton's principle (3) total energy of the structure at the same moments of time. In order to identify the tendency of total energy changes in the presence of increasing control action, those patches at:

b) $\varepsilon = -0.0188$, $K_g = 5$, c) $\varepsilon = -0.0303$, $K_g = 10$, d) $\varepsilon = -0.0422$, $K_g = 16$, e) $\varepsilon = -1.2710$, $K_g = 16.7$ are displayed in Figures 9(a), 9(b), 9(c) and 9(d) respectively.

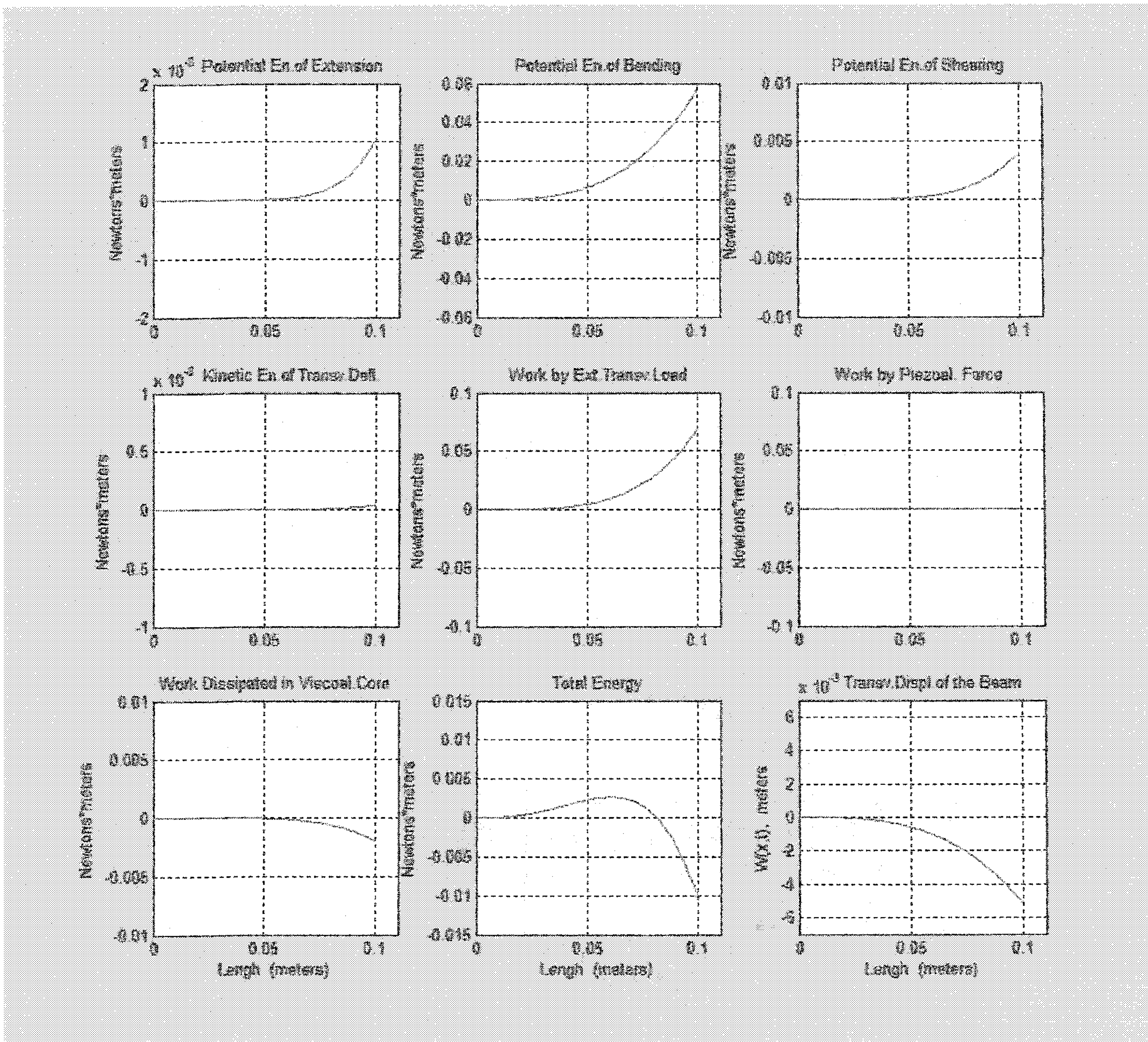

Figure 8. Energies at the dynamic motion (at $\varepsilon = 0, K_g = 0$).

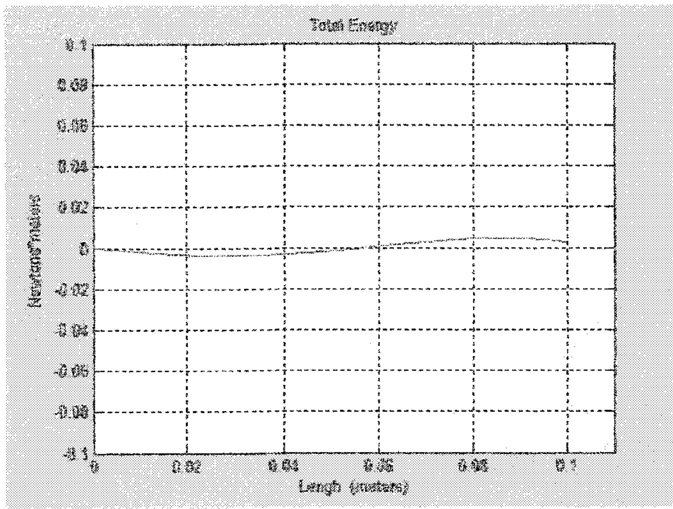

b) $\varepsilon = -0.0188, \quad K_g = 5$

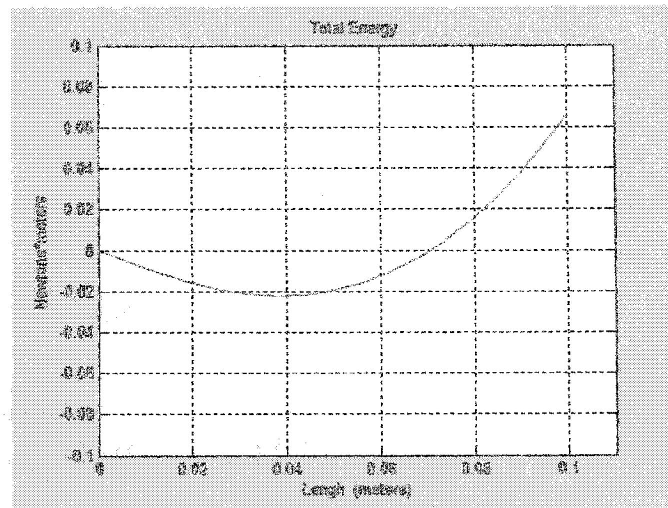

c) $\varepsilon = -0.0303, \quad K_g = 10$

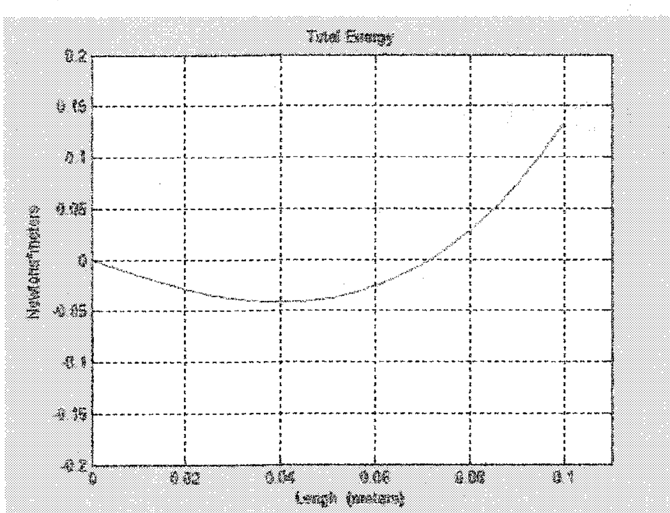

d) $\varepsilon = -0.0422, \quad K_g = 16$

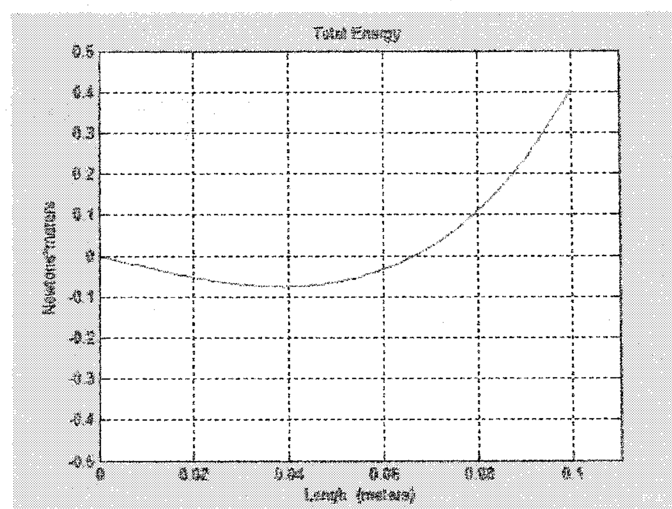

e) $\varepsilon = -1.2710, \quad K_g = 16.7$

Figure 9. Total energy at the dynamic motion.

For values $K_g \leq 16$ the path of total energy takes on a bent form with a greater slope for stronger control force, and the complete spatial integral of the total energies thoroughly the beam length at any moment of time is zero. It shows a good agreement with the principle of conservation of energy and proves the stability of the system at those conditions [38]. By contrast, values K_g>16 (the last example $\varepsilon = -1.2710$, $K_g = 16.7$) indicate clearly the unstable motion with significant total rate of altitudinal growth of energy.

CHAPTER 6

CONTROLLABILITY

6.1. EQUIVALENT STATE-SPACE REPRESENTATION

The system of equations of motion (12)-(17) has an equivalent state-space representation that can be determined by direct inspection of partial differential equations using Laplace transform. In particular, taking the Laplace transform with respect to one of the two variables gives an ordinary differential equation for the transform of the unknown function. This is so since the derivatives of this function with respect to the other variable slip into the transformed equation. In the latter also incorporates the given boundary and initial conditions.

Such a solution is possible considering that each of the independent variables x and t ranges over the positive axes (E. Kreyszig [18]).

6.2. SPACE-CONTINUOUS CONTROLLABILITY

6.2.1. *State-Space Form*

The use of Laplace transform of the system (12)-(17) with respect to t at first, will simplify the problem allocating the analysis on the space dependent controllability problem.

By applying the transforms of derivatives, subjects to the boundary conditions (16-17) and specified zero initial conditions:

$$L\left[\frac{\partial^2 w(x,t)}{\partial t^2}\right] = S^2 L[w(x,t)] - Sw(x,0) - \frac{\partial w(x,0)}{\partial t} = S^2 W(x,S),$$

where S is the Laplace transform variable.

Assuming that integration and differentiation may be interchanged (E.Kreyszig [18]):

$$L\left[\frac{\partial^2 u_1(x,t)}{\partial x^2}\right] = \int_0^\infty e^{-St} \frac{\partial^2 u_1(x,t)}{\partial x^2} dt = \frac{\partial^2}{\partial x^2} \int_0^\infty e^{-St} u_1(x,t) dt = \frac{\partial^2}{\partial x^2} L[u_1(x,t)] = U_{1xx}(x,S) \ ,$$

$$L\left[\frac{\partial^2 u_3(x,t)}{\partial x^2}\right] = \int_0^\infty e^{-St} \frac{\partial^2 u_3(x,t)}{\partial x^2} dt = \frac{\partial^2}{\partial x^2} \int_0^\infty e^{-St} u_3(x,t) dt = \frac{\partial^2}{\partial x^2} L[u_3(x,t)] = U_{3xx}(x,S) \ ,$$

$$L\left[\frac{\partial^2 w(x,t)}{\partial x^2}\right] = \int_0^\infty e^{-St} \frac{\partial^2 w(x,t)}{\partial x^2} dt = \frac{\partial^2}{\partial x^2} \int_0^\infty e^{-St} w(x,t) dt = \frac{\partial^2}{\partial x^2} L[w(x,t)] = W_{xx}(x,S) \ ,$$

$$L\left[\frac{\partial^4 w(x,t)}{\partial x^4}\right] = \int_0^\infty e^{-St} \frac{\partial^4 w(x,t)}{\partial x^4} dt = \frac{\partial^4}{\partial x^4} \int_0^\infty e^{-St} w(x,t) dt = \frac{\partial^4}{\partial x^4} L[w(x,t)] = W_{xxxx}(x,S) \ .$$

Thus, the Laplace transform of system (12)-(14) with respect to the t variable is given by

$$-K_1 U_{1xx} + \frac{G_2}{h_2}\left(U_1 - U_3 + hW_x\right) = 0 \ , \tag{33}$$

$$-K_3 U_{3xx} + \frac{G_2}{h_2}\left(U_1 - U_3 + hW_x\right) = 0 \ , \tag{34}$$

$$DW_{xxxx} + mS^2 W + \frac{G_2 h}{h_2}\left(U_{1x} - U_{3x} + hW_{xx}\right) = 0 \ . \tag{35}$$

Introducing auxiliary variable $V = U_1 - U_3$, the system (33)-(35) is written as follows:

$$V'' = \frac{G_2}{h_2}\left(\frac{1}{K_1} + \frac{1}{K_3}\right)\left(V + hW'\right),$$

$$W'''' = \frac{G_2 h}{Dh_2}\left(V' + hW''\right) - \frac{m}{D} S^2 W + \frac{Q}{D} \ .$$

Introducing the state variables:

$$z_1(x) = V(x,S),$$

$$z_2(x) = \frac{\partial}{\partial t} V(x,S) = \dot{V}(x,S),$$

$$z_3(x) = W(x,S),$$

$$z_4(x) = \frac{\partial}{\partial t} W(x,S) = \dot{W}(x,S),$$

$$z_5(x) = \frac{\partial^2}{\partial t^2} W(x,S) = \ddot{W}(x,S),$$

$$z_6(x) = \frac{\partial^3}{\partial t^3} W(x,S) = \dddot{W}(x,S),$$

equations of the motion take the following state-space representation:

$$\begin{bmatrix} \dot{z}_1 \\ \dot{z}_2 \\ \dot{z}_3 \\ \dot{z}_4 \\ \dot{z}_5 \\ \dot{z}_6 \end{bmatrix} = \mathbf{A} \begin{bmatrix} z_1 \\ z_2 \\ z_3 \\ z_4 \\ z_5 \\ z_6 \end{bmatrix} + \mathbf{B} Q, \tag{36}$$

where A and B are the state and input matrixes defined as:

$$\mathbf{A} = \begin{bmatrix} 0 & 1 & 0 & 0 & 0 & 0 \\ (1/K_1 + K_3)G_2/h_2 & 0 & 0 & (1/K_1 + 1/K_3)G_2 h/h_2 & 0 & 0 \\ 0 & 0 & 0 & 1 & 0 & 0 \\ 0 & 0 & 0 & 0 & 1 & 0 \\ 0 & 0 & 0 & 0 & 0 & 1 \\ 0 & G_2 h/(D h_2) & -mS^2/D & 0 & G_2 h^2/(D h_2) & 0 \end{bmatrix},$$

$$\mathbf{B} = \begin{bmatrix} 0 \\ 0 \\ 0 \\ 0 \\ 0 \\ 1/D \end{bmatrix},$$

Q is Laplace transform of the external transform load taken with respect to the t variable.

6.2.2. *Computation of Controllability*

The system given by equation (36) is state controllable if the vectors $\mathbf{B}, \mathbf{AB}, \ldots, \mathbf{A}^5\mathbf{B}$ are linearly independent, or the controllability matrix

$$\mathbf{M}_x = [\mathbf{B} \vdots \mathbf{AB} \vdots \mathbf{A}^2\mathbf{B} \vdots \mathbf{A}^3\mathbf{B} \vdots \mathbf{A}^4\mathbf{B} \vdots \mathbf{A}^5\mathbf{B}] \tag{37}$$

is not singular [22,30].

Appendix E presents calculation of both the controllability matrix (37) and determinant corresponding to it using symbolic notation. According to the results, the matrix $\mathbf{M}$ has a full rank 6 since $\det(\mathbf{M}) = \left(\frac{1}{K_1} + \frac{1}{K_3}\right)^3 G_2^3 h^2 \Big/ \left(D^2 h_2\right)^3$,

and, consequently, in the light of the spatial analysis, the system is controllable with given exciting transverse force .

6.3. TIME-CONTINUOUS CONTROLLABILITY

6.3.1. *State-Space Form*

The next step is allocated analysis of the time dependent controllability problem. Applying transforms of derivatives with respect to the x variable subjected to the boundary conditions (16),(17):

$$L[u_{1xx}(x,t)] = R^2 U_1(R,t) - E(R,t) \, ,$$

$$L[u_{3xx}(x,t)] = R^2 U_1(R,t) \, ,$$

$$L[w_{xx}(x,t)] = R^2 W(R,t) \, ,$$

$$L[w_{xxxx}(x,t)] = R^4 W(R,t) \, ,$$

where R is the Laplace transform variable.

Assuming that integration and differentiation may be interchanged:

$$L\left[\frac{\partial^2 w(x,t)}{\partial t^2}\right]=\int_0^\infty e^{-Rx}\frac{\partial^2 w(x,t)}{\partial t^2}dx=\frac{\partial^2}{\partial t^2}\int_0^\infty e^{-Rx}w(x,t)dx=\frac{\partial^2}{\partial t^2}L[w(x,t)]=\frac{\partial^2}{\partial t^2}W(R,t)\,.$$

Now the equations of the motion (12)-(14) can be written as follows:

$$-K_1R^2U_1+K_1E+\frac{G_2}{h_2}\left(U_1-U_3+hRW\right)=0\,, \tag{38}$$

$$-K_3R^2U_3-\frac{G_2}{h_2}\left(U_1-U_3+hRW\right)=0\,, \tag{39}$$

$$DR^4W+m\frac{\partial^2 W}{\partial t^2}-\frac{G_2hR}{h_2}\left(U_1-U_3+hRW\right)-Q=0\,. \tag{40}$$

From the first two equations (38),(39) of the system:

$$U_1=\frac{E}{R^2}-\frac{K_3}{K_1}U_3\,. \tag{41}$$

Substituting (41) into equation (39) yields

$$U_3=\frac{K_1\left(E+hR^3W\right)}{R^2\left(K_1+K_3-h_2K_1K_3R^2/G_2\right)}\,. \tag{42}$$

Substituting equations (41) and (42) into equation (40) allows elimination of functions U_1 and U_3 from the third equation of the system:

$$\begin{aligned}&m\frac{\partial^2 W}{\partial t^2}-\left[\frac{G_2^2R^2}{K_1K_3R^2/(K_1+K_3)-G_2/h_2}-DR^4\right]W+\\&+\frac{G_2h}{h_2R}\left[\frac{G_2-1}{G_2-h_2K_1K_3R^2/(K_1+K_3)}\right]E-Q=0\end{aligned}\,, \tag{43}$$

where, E and Q are Laplace transforms of two inputs ε and q.

Defining state variables $z_1(t)$ and $z_2(t)$ as

$$z_1(t)=W(R,t)\,,\qquad z_2(t)=\frac{\partial}{\partial t}W(R,t)=\dot{W}(R,t)\,,$$

the equation (43) can be given by the following state-space representation:

$$\begin{bmatrix} \dot{z}_1 \\ \dot{z}_2 \end{bmatrix} = \begin{bmatrix} 0 & 1 \\ P/m & 0 \end{bmatrix} \begin{bmatrix} z_1 \\ z_2 \end{bmatrix} + \begin{bmatrix} 0 \\ -T/m + Q/(mE) \end{bmatrix} E \,, \tag{44}$$

where

$$P = \frac{G_2^2 R^2}{K_1 K_3 R^2/(K_1 + K_3) - G_2/h_2} - DR^4 \,, \qquad T = \frac{G_2 h}{h_2 R}\left[\frac{G_2 - 1}{G_2 - h_2 K_1 K_3 R^2/(K_1 + K_3)}\right]$$

and Q, E are Laplace transforms of transverse and piezoelectric loads taken with respect to the x variable.

6.3.2. *Component Controllability*

In the two-input motion described by equations(36)-(38), it is useful to determine the controllability of a system relative to the individual components of its input. Such a determination would be important, for example, if one of the actuators were to fail.

Disregarding the piezoelectric input, equation (38) can be defined by the state-space representation

$$\begin{bmatrix} \dot{z}_1 \\ \dot{z}_2 \end{bmatrix} = \begin{bmatrix} 0 & 1 \\ P/m & 0 \end{bmatrix} \begin{bmatrix} z_1 \\ z_2 \end{bmatrix} + \begin{bmatrix} 0 \\ 1/m \end{bmatrix} Q \,.$$

The controllability matrix

$$\mathbf{M}_{tq} = \begin{bmatrix} 0 & 1/m \\ 1/m & 0 \end{bmatrix}$$

has full rank 2, so the entire state is controllable using the only input of transverse load.

Next, suppose the given system has the only piezoelectric input, then the resulting state-space representation is obtained by

$$\begin{bmatrix} \dot{z}_1 \\ \dot{z}_2 \end{bmatrix} = \begin{bmatrix} 0 & 1 \\ P/m & 0 \end{bmatrix} \begin{bmatrix} z_1 \\ z_2 \end{bmatrix} + \begin{bmatrix} 0 \\ -T/m \end{bmatrix} E \,.$$

In this case, the controllability matrix

$$\mathbf{M}_{t\varepsilon}=\begin{bmatrix}0 & -T/m \\ -T/m & 0\end{bmatrix}$$

has nonzero determinant that shows the complete state control is possible by piezoelectric actuator alone if the external transverse loads were to fail.

6.3.3. *Stabilisability*

Finally, consider the system defined by equation (39) with both inputs. In view of canonical form the state-space representation of equation (39) can be written

$$\begin{bmatrix}\dot{\hat{z}}_1 \\ \dot{\hat{z}}_2\end{bmatrix}=\begin{bmatrix}-\sqrt{P/m} & 0 \\ 0 & \sqrt{P/m}\end{bmatrix}\begin{bmatrix}\hat{z}_1 \\ \hat{z}_2\end{bmatrix}+\begin{bmatrix}Q/(mE)-T/m \\ (Q/(mE)-T/m)\sqrt{P/m}\end{bmatrix}E\ , \tag{45}$$

with eigenvalues $\lambda_1=-\sqrt{P/m}$, $\lambda_2=\sqrt{P/m}$ and a basis of eigenvectors $\begin{bmatrix}1 & -\sqrt{P/m}\end{bmatrix}^T$, $\begin{bmatrix}1 & \sqrt{P/m}\end{bmatrix}^T$.

Since the controllability matrix of the system (40)

$$\mathbf{M}_t=\begin{bmatrix}Q/(mE)-T/m & (Q/(mE)-T/m)\sqrt{P/m} \\ (Q/(mE)-T/m)\sqrt{P/m} & (Q/(mE)-T/m)P/m\end{bmatrix}$$

is singular, it follows, the system can not be completely state controlled. However, in this partially controllable system the both stable and unstable modes that correspond to the eigenvalues $\lambda_1=-\sqrt{P/m}$ and $\lambda_2=\sqrt{P/m}$ withstand control inputs. Such system can be made stable by the use of a suitable feedback. Thus, the system is stabilizable.

CHAPTER 7

STABILITY

7.1. LYAPUNOV STABILITY ANALYSIS

Lyapunov's direct method is a powerful tool for stability analysis, since the approach does not require that we integrate the equations of motion and the method can be applied to higher dimensional nonlinear systems. Designing a controller for the nonlinear system given by (26)-(31), suppose that the objective is to transfer every possible initial state to some specified equilibrium. The extent to which this goal is accomplished is determined by the set of initial states that actually do get transferred to the target state.

Consider the dynamic system of the present study in the usual form

$$\dot{\overline{X}} = \bar{f}(\overline{X},t),$$

where,

$$\overline{X} = [x_1, x_2, x_3, x_4, x_5, x_6]^T = [u_1 - u_3, u_{1x} - u_{3x}, w, w_x, w_{xx}, w_{xxx}]^T$$

and x_i, $i = 1 \ldots 6$, are function of time. It is clear, from the boundary conditions, that $\bar{f}(\overline{0},t) = \overline{0}$ for all t. Assume that $\hat{X}(x,t)$ is a locally asymptotically stable equilibrium solution. For the system described by (26)-(31) implemented boundary control strategy implies the dependence of every state upon strain induced by piezoelectric, therefore, the equilibrium state is also function of ε. The problem is to determine (or estimate) the domain of attraction to $\hat{X}(x(\varepsilon),t)$.

Lyapunov's main attractor stability theorem provides a sufficient condition for asymptotic stability (T.Vincent [43]). If there exists a continuously differentiable function $V(\overline{X},t)$, bounded in the region D ($V \subseteq D$) and satisfying the conditions: $V(\overline{X},t)$ is positive-definite and the time derivative of this function, $\dot{V}(\overline{X},t)$, is negative-definite, then the equilibrium state at the origin is asymptotically stable. If, however, there exists a positive-definite function $V(\overline{X},t)$ such that $\dot{V}(\overline{X},t)$ is identically zero, then the system can remain in a limit cycle. The equilibrium state, in this case, is said to be stable in the sense of Lyapunov (T.L.Vincent [43], F.Lewis [23], K.Ogata [30]).

In the current analysis the total energy of the system is a good candidate for a Lyapunov's function that can be used to estimate the domain of attraction. In accordance with a principle of conservation of energy the total energy E of the beam/ACLD system is obtained using equations (4)-(10) as follows:

$$E = U_1 + U_2 + U_3 + T - (W_1 + W_2 + W_3) = Const_1,$$

where, $|Const_1| \leq D$.

Defining a scalar function by $V(\overline{X}) = E + Const_2$, where $|Const_1| < Const_2$, which is positive-definite, then the time derivative of this function along any trajectory is:

$$\frac{\partial}{\partial t}V = \frac{\partial}{\partial t}(U_1 + U_2 + U_3 + T) - \frac{\partial}{\partial t}(W_1 + W_2 + W_3). \qquad (46)$$

It has been shown (A.Baz [9]) the first term in the expression (46) gives:

$$\dot{U}_1 + \dot{U}_2 + \dot{U}_3 + T = bK_1 u_{1t}(L)\varepsilon - (G_2'\eta h_2 b/\omega)\int_0^L \gamma_t^2 dx \;. \qquad (47)$$

Substituting equations (8)-(11) and (47) into equation (46) yields: $\frac{\partial}{\partial t}V =$

$$= bK_1 u_{1t}(L)\varepsilon - (G_2'\eta h_2 b/\omega)\int_0^L \gamma_t^2 dx - b\frac{\partial}{\partial t}\int_0^L qw dx - bK_1\frac{\partial}{\partial t}\int_0^L \varepsilon u_{1x} dx + h_2 bG_2'\eta\frac{\partial}{\partial t}\int_0^L \frac{\gamma_t\gamma}{\omega}dx \quad (48)$$

Considering the last three terms in the equation (48):

$$b\frac{\partial}{\partial t}\int_0^L qw\,dx = b\int_0^L (q_t w + q w_t)\,dx\,, \tag{49}$$

$$\frac{\partial}{\partial t}\int_0^L \varepsilon u_{1x}\,dx = \frac{\partial}{\partial t}\varepsilon\left(u_1(L)-u_1(0)\right) = \frac{\partial}{\partial t}\left(\varepsilon u_1(L)\right) = \frac{\partial}{\partial t}\left(\varepsilon^2 L\right) = 2L\varepsilon\varepsilon_t = 2u_{1t}(L)\varepsilon\ , \tag{50}$$

$$(h_2 bG_2'\eta/\omega)\frac{\partial}{\partial t}\int_0^L \gamma_t\gamma\,dx = \left(h_2 bG_2'\eta/\omega\right)\int_0^L (\gamma_t^2 + \gamma_{tt}\gamma)\,dx\ . \tag{51}$$

Substituting equations (49)-(51) into (48), it reduces to:

$$\dot{V} = -bK_1 u_{1t}(L)\varepsilon - b\int_0^L (q_t w + q w_t)\,dx + \left(h_2 bG_2'\eta/\omega\right)\int_0^L \gamma_{tt}\gamma\,dx\,. \tag{52}$$

In order for the function $\dot{V}$ expressed by (52) to be negative-definite, that is the same as providing the asymptotic stability of the equilibrium state, the following necessary and sufficient condition for piezoelectric control action is required:

$$\varepsilon \le \varepsilon^{opt}\,,$$

where,

$$\varepsilon^{opt} = -\frac{1}{K_1 u_{1t}(L)}\left[\int_0^L (q_t w + q w_t)\,dx - \left(h_2 G_2'\eta/\omega\right)\int_0^L \gamma_{tt}\gamma\,dx\right]. \tag{53}$$

Figure 10 shows the stability boundary and displacement contours plotted in (ε, w) plane. Displayed also in the Figure 10 is the optimal combination of control force ε and control gain K_g at which the displacement attains the minimum. At this point the optimal control gain K_g^{opt} can be evaluated.

It is important here to note that the choice of the active control action ε establishes the stability (or unstability in the case of symbol > in the expression above) of the motion.

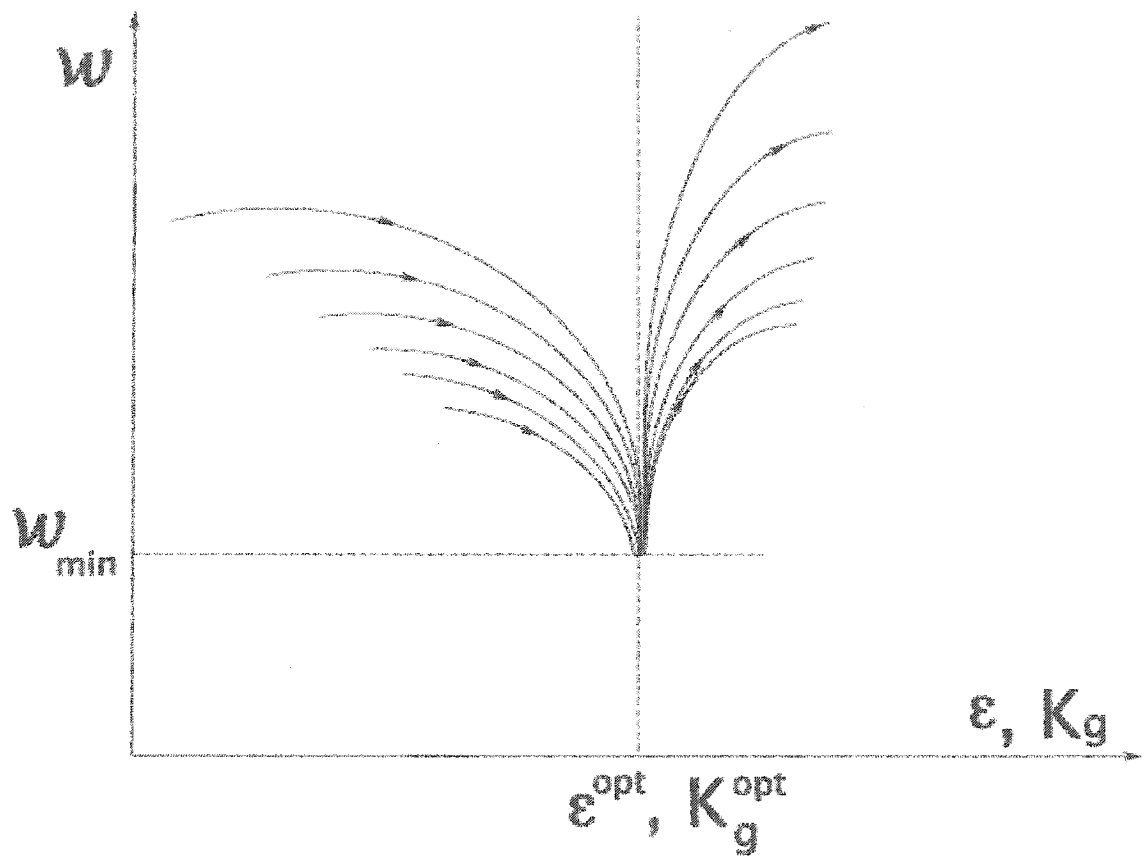

Figure 10. The stability boundary and displacement contours of the beam/ACLD system in the (ε, w) plane.

The terms of equation (52) provide quantitative means for weighing the individual contributions of ACLD (the first term), the external transverse loads (the second term) and the PCLD (the third term) to the total rate of energy dissipation of the beam system. Hence, the stability of the system is attributed to the balance and interaction of three of these processes in the beam/ACLD treatment, and the process depends on the choice of the active control action ε, as it is expressed by inequity (53).

7.2. PHASE PLANE ANALYSIS

The graphical representation of the nature of the system response corresponding to various time initial conditions at the end point of the beam is directly displayed on the phase plane portraits in three dimensional planes shown in Figure 11. The graphs are constructed by the program and block diagram (Appendixes F and G) working in animated regime.

It is seen from the phase portraits that trajectories of the system move in a closed periodic patterns for gains of the controller K_g <15.5 that corresponds to the orbitally stable state of the system. Starting from K_g around 15.5, an effect of small beating vibrations that decay with time is noticeable, that indicates the phase of the asymptotically orbitally stable solution.

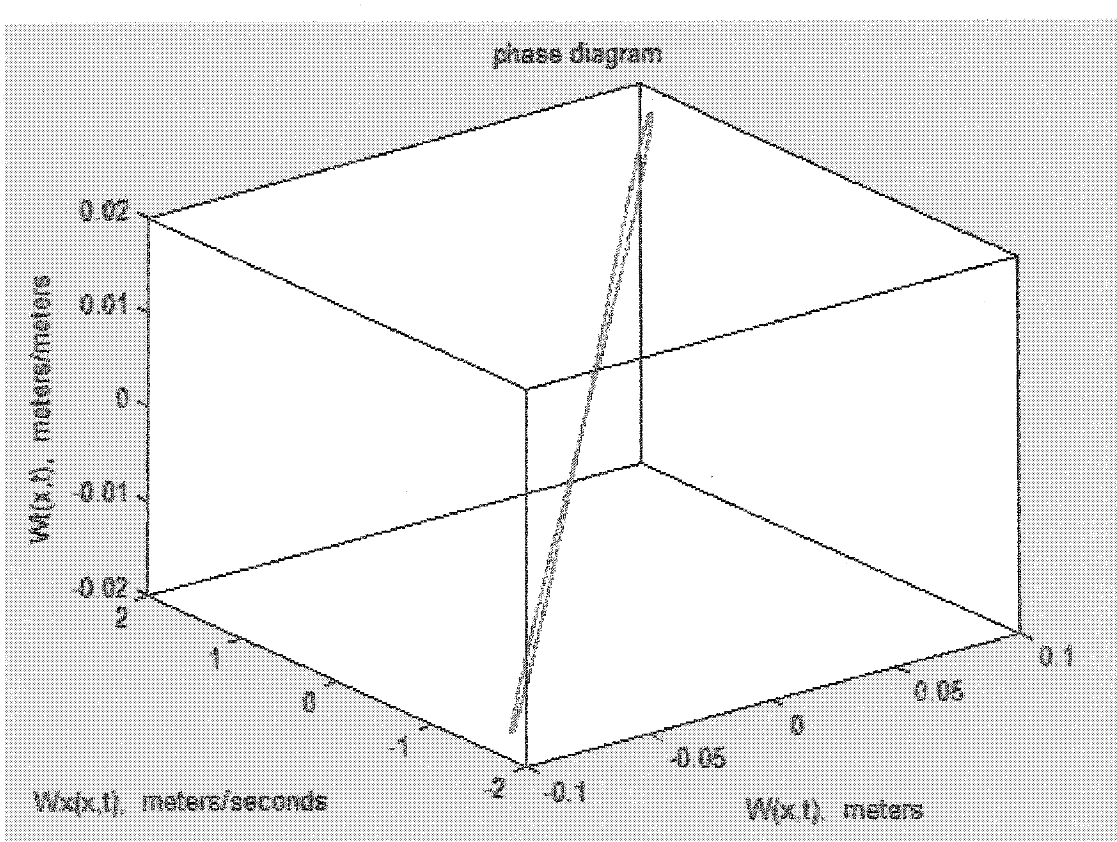

a)

Figure 11. Phase plane portraits of the system. a) $\varepsilon = 0$, $K_g = 0$ (stable motion)

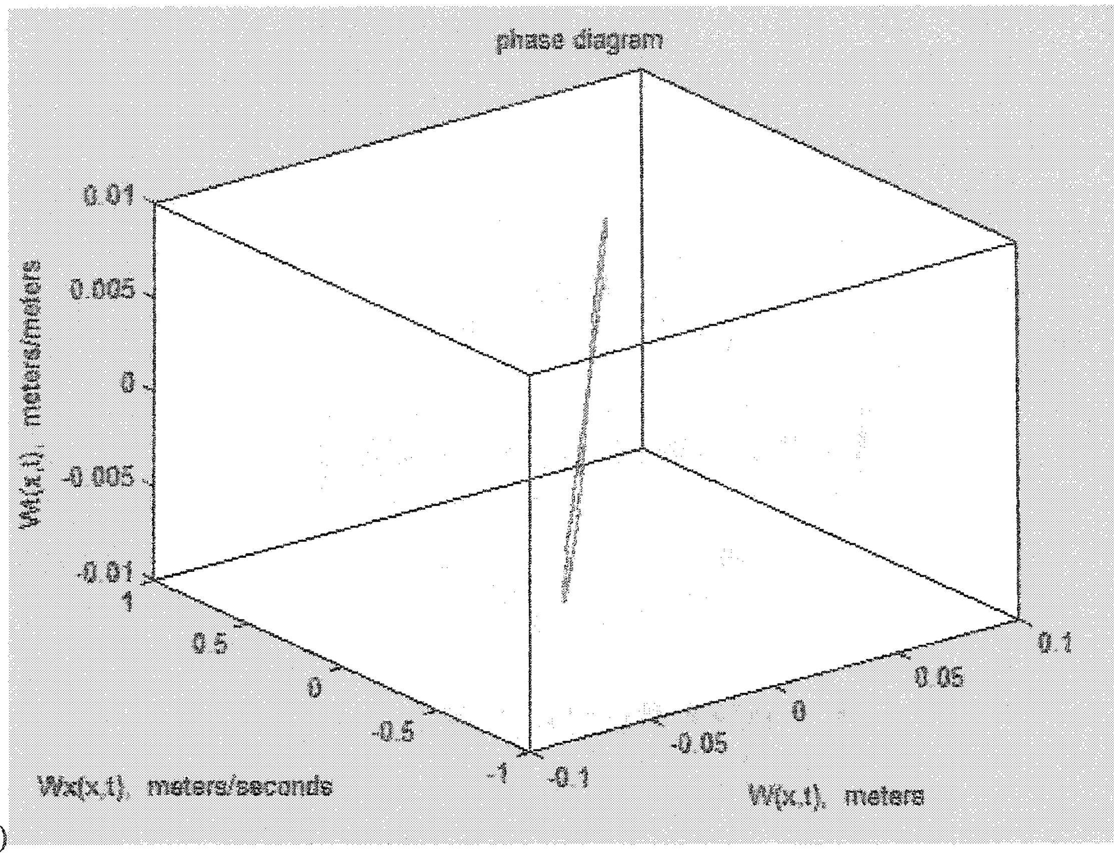

b)

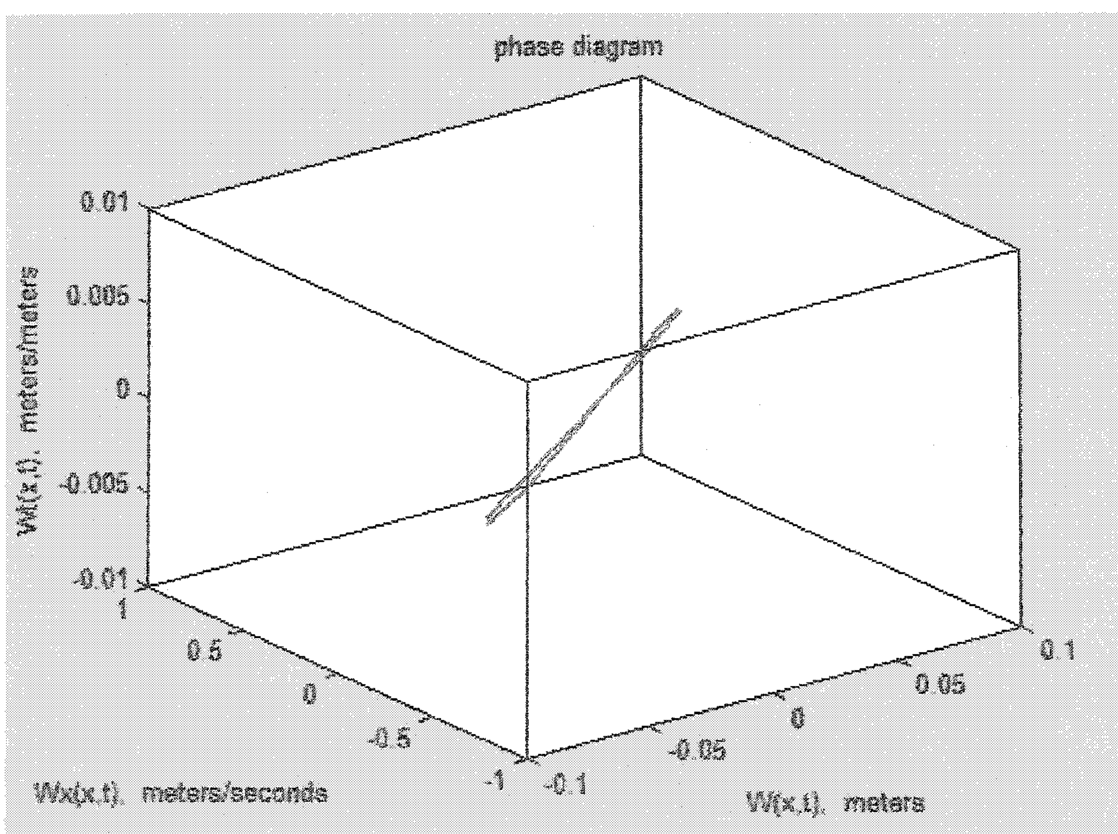

c)

Figure 11. Phase plane portraits of the system: b) $\varepsilon = -0.0303$, $K_g = 10$ (stable motion); c) $\varepsilon = -0.0388$, $K_g = 15.5$ (asymptotically stable motion);

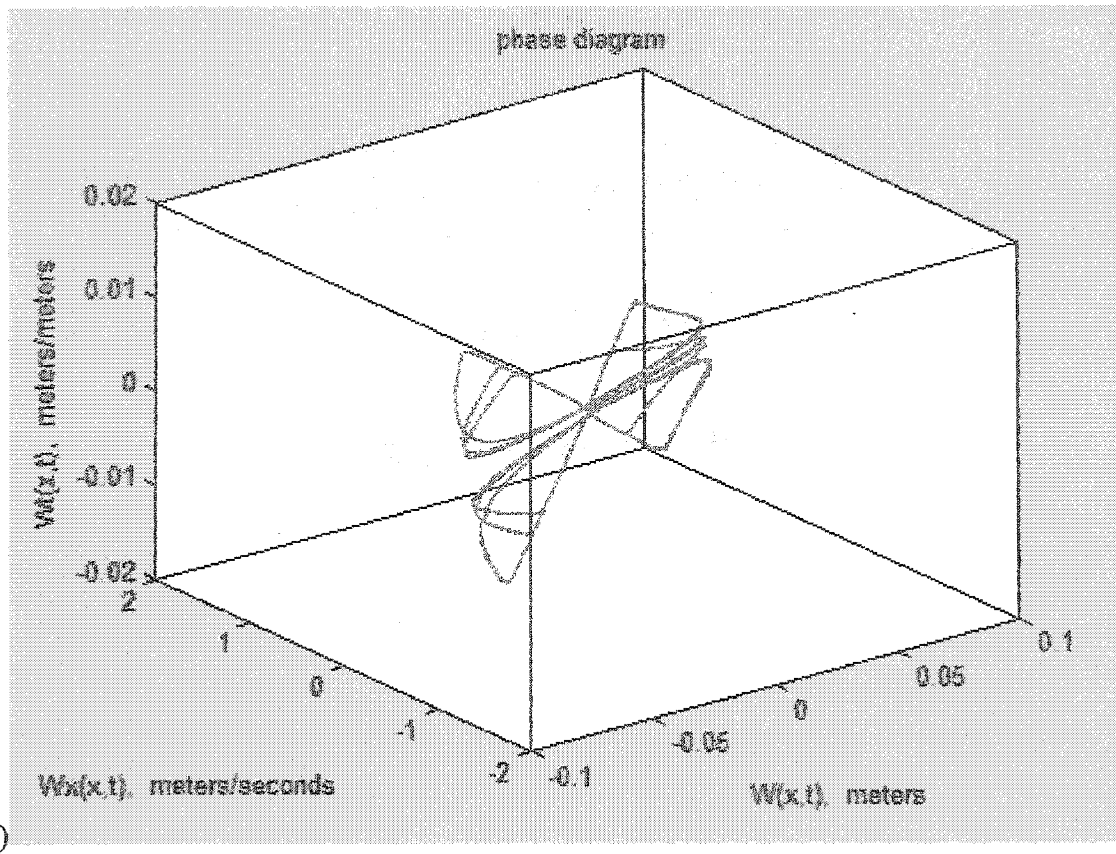

d)

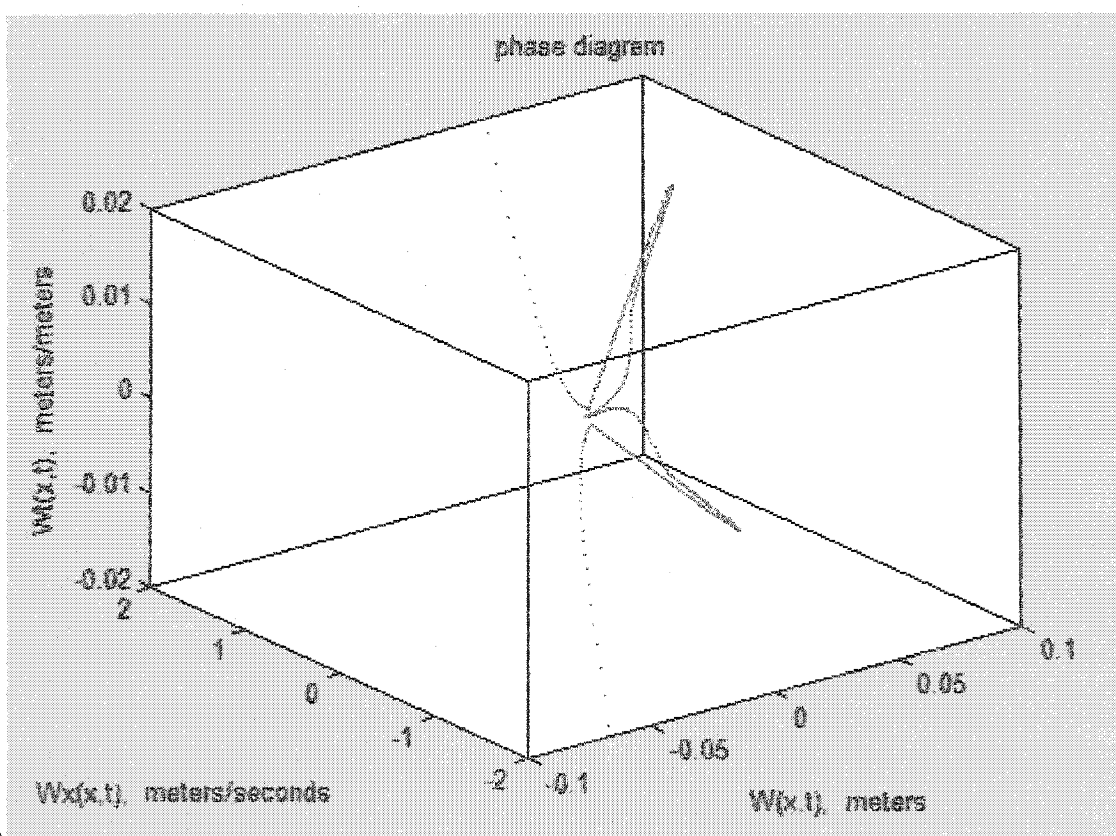

e)

Figure 11. Phase plane portraits of the system: d) $\varepsilon = -0.0422, K_g = 16$ (critical asymptotically stable motion); e) $\varepsilon = -1.2710, \quad K_g = 16.7$ (unstable motion).

A critical case occurs if the control gain has value $K_g = 16$: the movement is not periodic, the increase of beating alternates with its decrease, but the trajectories still vibrate in the limited area. Finally, at K_g>16, the system becomes unstable since the trajectories can not approach to the limited orbits anymore.

Thus, determination of the domain of attraction must rely on the quantitative amount of the controlling piezoelectric action ε, represented by the control gain parameter K_g: the set of initial states $\overline{X}(x_0, t_0)$ with controller gains $K_g \leq 16$ from which solutions $\overline{X}(x,t)$ converge to $\hat{X}(x(\varepsilon),t)$ as $t \to \infty$, defines the domain of attraction D for asymptotically stable solution.

Comparing results, the rationale of the optimal control design of the beam/ACLD structure becomes clear from the geometry illustrated in the phase plane graphs.

CHAPTER 8

CONTROL DESIGN

In the context of signals, the process of control design is a disturbance rejection problem that defines a feedback controller which minimizes the maximum amplitude of the regulated output over disturbances of bounded magnitude [19]. The closed loop system shown in Figure 12 depicts a block diagram of a controller with transfer function K_g that stabilizes the ACLD/beam system with transfer function F in the presence of an external disturbance q.

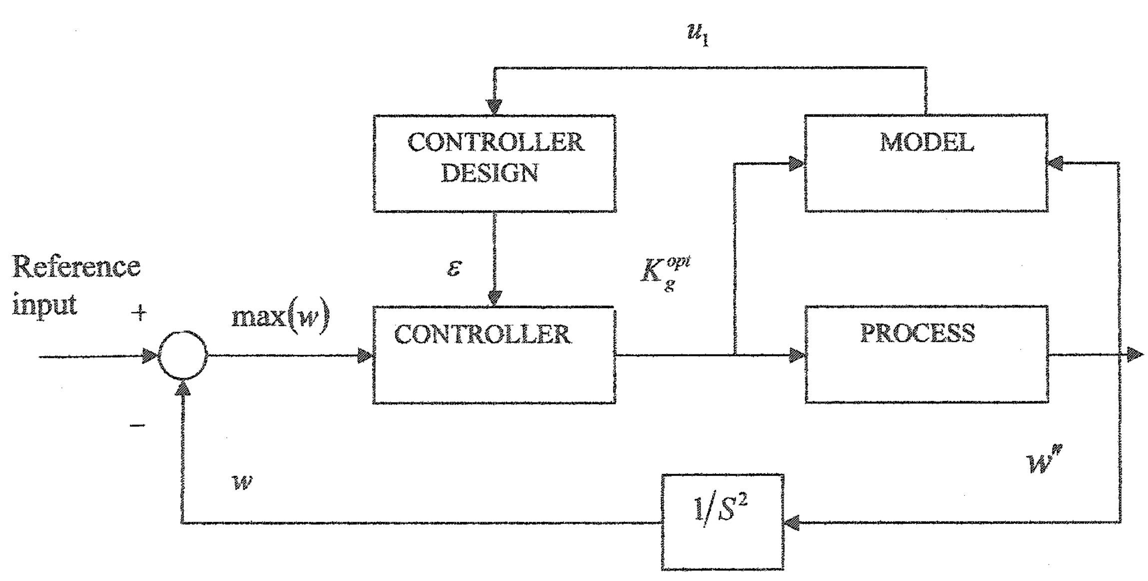

Figure 12. Block diagram of ACLD system with controller and external disturbance.

The key issue is the character of the disturbance represented by harmonic force, and, accordingly, the dynamics of the system are changing continuously. It is useful to compensate for these changes by changing the controller. Parameters of the controller can be adjusted via estimation of the process parameters. To initialize the continuous gain scheduling of the controller, the boundary control strategy, incorporated by boundary condition (17), performs the automatic tuning of such adaptive control procedure.

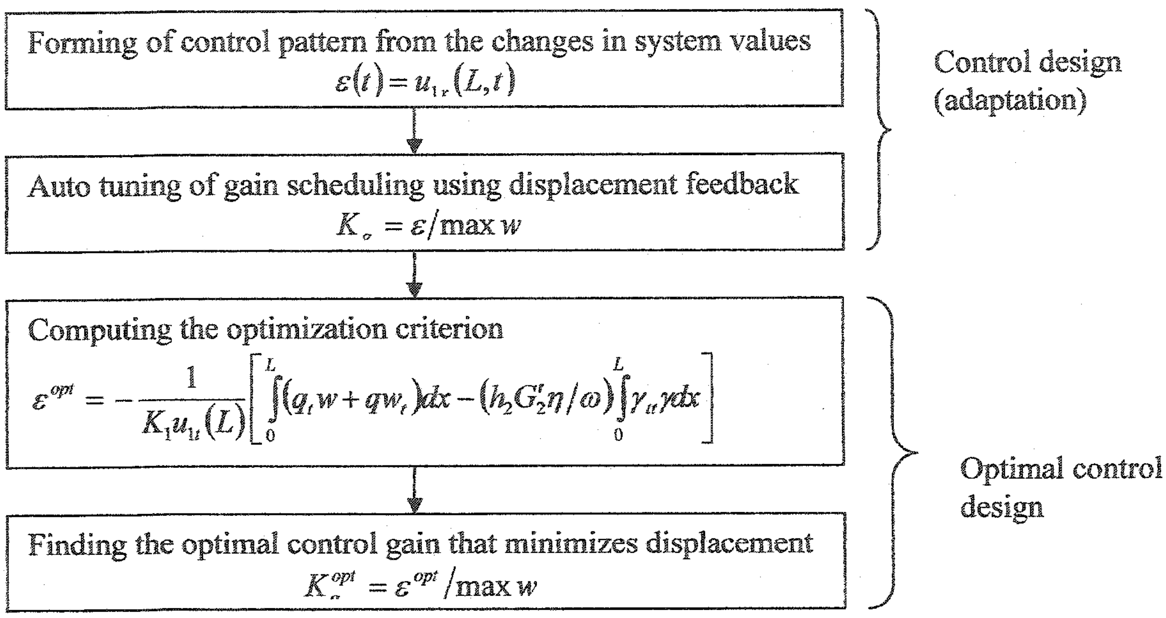

Figure 13. Adaptive optimal control design scheme.

The next is optimization problem of the ACLD treatment that aims at selecting the optimal control gain K_g^{opt} to minimize the stable altitudinal deflection of the base structure, subject to the harmonic excitation, using displacement feedback control action (32). Mathematically, it is formulated as: find gain $K_g\left(\varepsilon^{opt}, \max(w), u_1, u_3, \gamma\right)$ to minimize the amplitude of transverse displacement w, such as the system reminds stable and the configuration of the system is known. The direct optimization criterion is focused on the stability assessment (53). Thereby, two control objectives, effective attenuation of load disturbances and robust set point following, are of primary concern for optimal process.

The main design principle can be well described by a model shown in Figure 13.

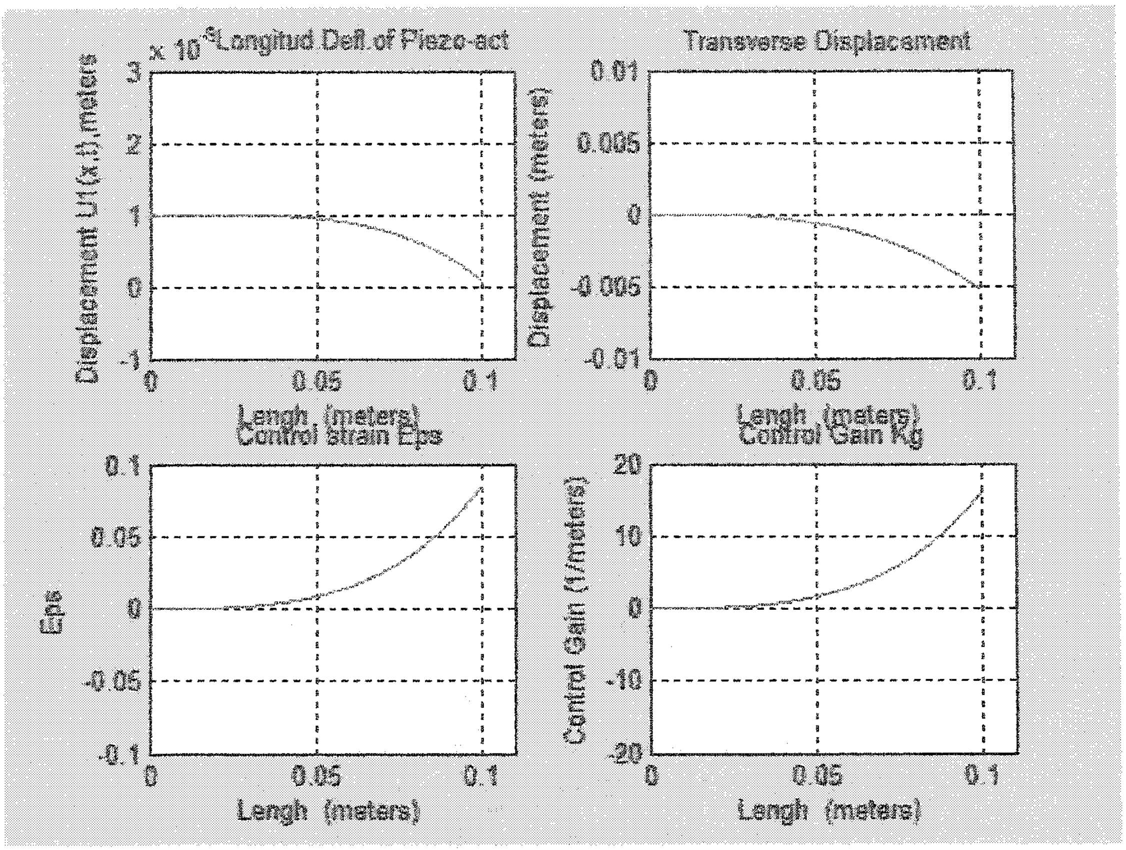

Figure 14. Distributions of displacements, control strain and control gain of adaptive optimal controller.

Implementation of above control strategy for the beam/ACLD treatment given in Table 1 is simulated by the program and block scheme presented in Appendixes H, I respectively. Figure 14 demonstrates the continuously changing values of displacements u_1, w and corresponding changing of constrain ε with auto tuning control gain K_g. Obtained optimal control gain is $K_g^{opt} = 16.0465$. It matches well with the results determined in Sections 3.3 and 5.2 when starting from about the same value, the suppressed attenuation of displacement of the system monitored the transitional stage to excessive vibrations. Hence, the analysis indicates, the applicability of the controller has been effective in damping out vibrations with control gain favorably close from the left to its optimum.

CHAPTER 9

CONCLUSIONS

The current study extends the initial work of A.Baz [9-11,31-32, and 34-37] on dynamics and optimal attenuation of flexural vibrations of elastic beams which are fully covered with active and passive constrained damping layers. The equations of motion and boundary conditions governing the performance of this class of surface treatments are based on variational formulation of kinematics of the beam/ACLD system using Hamilton's principle. The harmonic response of the cantilever beam is evaluated in time-domain for different values of the constraining action. The optimization problem is conducted to find the adaptive optimal control gains of the piezoelectric actuator to minimize the flexural deflection of the base layer using stability criteria.

This investigation presents the following innovative physical applications of mathematical theory:

1) Solution of the system equations is obtained by a combined variational (shear strain function) and modal (all displacements) analysis.
2) The use of continuous spatial response simulation in the Control Toolbox of Matlab-Simulink instead of conventional time-integration technique.
3) Application of two dimensional Laplace transforms theory for the controllability inspection.
4) Phase plane 3-dimentional demonstration of the stability.

Automated numerical programs that have been developed for designing tree-layer beams exhibit time-spatial solutions of the problems in the dynamic regime.

The validity of the model is checked for constrained layered beam arrangements using data available in the literature. Numerical results are carried out, to highlight the influence of various values of constraining action. The proposed analytical design of the adaptive optimal control of the piezo-actuator is compared with other calculations obtained by model simulation. Results are observed to match with good accuracy.

Based on the results in this study, the following conclusion may be drawn.

1) Application of the ACLD treatment with the boundary controller presented is effective while the control gain of the actuator does not exceed a particular value.
2) Such optimal value of the control action is attained as an optimal balance between constraining and external load efforts, passive constrained and structural damping.
3) Amplitude attenuation of about 52% for the first vibration mode was achieved.
4) Although the boundary controller is shown to be theoretically stable in response to one of the two input components, which are external transverse load and the piezoelectric action, the stability bounds are not infinite because of the combined actuator and disturbance dynamics.
5) By the use of an appropriate closed loop feedback the system with ACLD treatment is stabilizable.

The thesis suggests a generally analytical method for the adaptive optimal control design of the system behavior treated with ACLD. Most of existing models are developed for the robust control design on the basis of finite element formulation of the structure associated with frequency response analysis. This is somewhat different from the present Present technique. There are results could be compared qualitatively. According to [6,7] results, increasing of the flexural rigidity of the piezo-actuator predicts better constraining damping at the beginning and the failure of the controller at its high values. Studies [31,32] of plates and thin shells [11,45] mention that after the constraining strain parameter reaches a best value, further increasing on the contrary gives worse results. In [1] the optimal sizing of beam/ACLD treatment yields 54% amplitude attenuation for the first mode of vibrations. This is similar to the results presented in this approach. Numerical examples showed consistent results with our physical intuition.

Extension of this research can be performed to include attenuation of higher vibration modes in the optimal control analysis. An optimal scheme in conjunction with the other strain distributions such as piece-wise ACLD patches may invoke an interesting topic for the future research. Important experimental issues, including the damping performance measurements, are also under consideration.

For process control applications, the implemented here adaptive controller deserves a special mention. It is a powerful approach for dealing with varying disturbances, model uncertainties. The use of the described procedure for the optimal control design, adjusted to the changing dynamics of the ACLD structures, is in progress of this investigation.

The present work provides an application of analytical techniques used in design of nonlinear and optimal feedback control of the system. The fundamental topics of stability, controllability, and optimality are developed and presented in a unified fashion that establishes strong connections between all three topics.

While this investigation is helpful in setting up guidelines for ACLD designers, the new ideas developed here could be a good direction for future research constituting many engineering applications.

APPENDIX A

SOLUTION OF EQUATIONS OF MOTION

MATLAB Program

```
G21=350000;     nu=1.5;
H1=0.000625;    H2=0.0025;      H3=0.00125;
H=H2+H1/2+H3/2;
E1=63000000;    E3=206850000;
K1=E1/H1;       K3=E3/H3;
L=0.1;          H4=0.05*L;      B=0.1*L;
I1=B*((2*H1+2*H2+2*H3+H4)^3-(2*H2+2*H3+H4)^3)/12;
I3=B*(2*H3+H4)^3/3;
D=(E1*I1+E3*I3)/B;
m=0.05/(B*L);
WL=0.005;       QL=1000000;     n=1;
w=(n*pi)^2*sqrt((E1*I1+E3*I3)/(m*(H1+H2+H3)*B))/L^2;
wd=100;   f=wd/(2*pi);   Eps=0;
figure(1);  clf;
for ti = 2*pi:0.001:2.066*pi
    Qti=sin(wd*ti);
    Wti=QL*(ti*wd-sin(wd*ti))/(m*WL*wd^2);
    Wtti=QL*(1-cos(wd*ti))/(m*WL*wd);
    Wttti=QL*(sin(wd*ti))/(m*WL);
    [T,X,Y]=sim('Attachment2',[0,L]);
    displacement1=Y(:,1)-0.000000001;
    transverse_displacement=Y(:,2);
    displacement3=Y(:,3);
    shear_strain_Gamma=Y(:,4);
    zmax=max(Y(:,2));
    zmin=min(Y(:,2));
    if abs(zmax)>abs(zmin)
       z=sign(zmax);
       a=abs(zmax);
    else z=sign(zmin);
         a=abs(zmin);
    end;
%   Eps=-16.65*z*a;

subplot(2,2,1);
plot(T,displacement1); grid;
title('          Longitud.Defl.of Piezo-act.');
ylabel('Displacement U1(x,t),  (m)');
xlabel('Lengh   (meters)');
box on
axis([0 L+0.1*L -0.000000001 0.000000001]);
```

```
subplot(2,2,2);
plot(T,displacement3); grid;
title('          Longitud.Defl.of Beam/sen.');
ylabel('Displacement U3(x,t), (m)');
xlabel('Lengh  (meters)');
box on
axis([0 L+0.1*L -0.000000001 0.000000001]);

subplot(2,2,3);
plot(T,shear_strain_Gamma); grid;
title('        Shear Strain in Vis.-el. Layer');
ylabel('Shear strain Gamma(x,t), (m)');
xlabel('Lengh  (meters)');
box on
axis([0 L+0.1*L -0.3 0.3]);

subplot(2,2,4);
plot(T,transverse_displacement); grid;
title('          Transv.Displ.of the Beam');
ylabel('Transverse Displ. W(x,t), (m)');
xlabel('Lengh  (meters)');
box on
axis([0 L+0.1*L -0.007 0.007]);

WL=z*a;
end;
disp('max(transverse_displacement)=');max(transverse_displacement)
```

APPENDIX B

SOLUTION OF EQUATIONS OF MOTION

SIMULINK Block Diagram

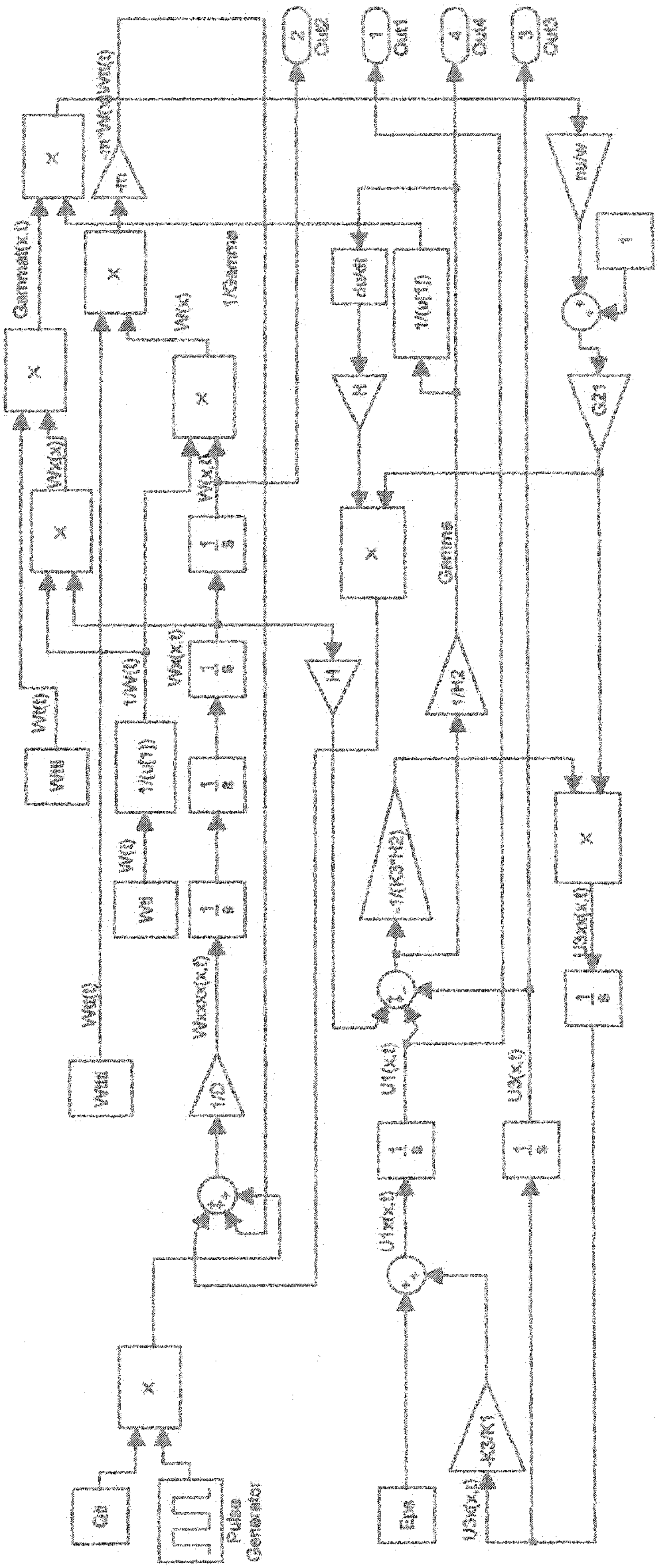

APPENDIX C

ENERGIES

MATLAB Program

```
G21=350000;          nu=1.5;
H1=0.000625;         H2=0.0025;          H3=0.00125;
H=H2+H1/2+H3/2;
E1=63000000;         E3=206850000;
K1=E1/H1;            K3=E3/H3;
L=0.1;               H4=0.05*L;          B=0.1*L;
I1=B*((2*H1+2*H2+2*H3+H4)^3-(2*H2+2*H3+H4)^3)/12;
I3=B*(2*H3+H4)^3/3;
D=(E1*I1+E3*I3)/B;
m=0.05/(B*L);
WL=0.005;            QL=1000000;          n=1;
w=(n*pi/L)^2*sqrt(E1*I1+E3*I3/(m*(H1+H2+H3)*B));
wd=100;              f=wd/(2*pi);         Eps=0;
figure(1); clf;
for ti = 2*pi:0.001:2.065*pi
    Qti=sin(wd*ti);
    Wti=QL*(wd*ti-sin(wd*ti))/(m*WL/wd^2);
    Wtti=QL*(1-cos(wd*ti))/(m*WL*wd);
    Wttti=QL*(sin(wd*ti))/(m*WL);
    [T,X,Y]=sim('Attachment4',[0,L]);
    displacement1=Y(:,1);
    transverse_displacement=Y(:,2);
    displacement3=Y(:,3);
    shear_strain_Gamma=Y(:,4);
    potential_energy_extension=Y(:,5);
    potential_energy_bending=Y(:,6);
    potential_energy_shearing=Y(:,7);
    kinetic_energy_transv_deflec=Y(:,8);
    work_external_transv_load=Y(:,9);
    work_piezoelectric_control_force=Y(:,10);
    work_dissipated_viscoelastic_core=Y(:,11);
    summary_energy=Y(:,12);
    zmax=max(Y(:,2));
    zmin=min(Y(:,2));
    if abs(zmax)>abs(zmin)
       z=sign(zmax);
       a=abs(zmax);
    else z=sign(zmin);
       a=abs(zmin);
    end;
    Eps=-16*z*a;

 subplot(3,3,1);
 plot(T,potential_energy_extension); grid;
 title('      Potential En.of Extension');
 ylabel('Newtons*meters');
 box on
 axis([0 L+0.1*L -0.00000002 0.00000002]);
 subplot(3,3,2);
 plot(T,potential_energy_bending); grid;
 title('Potential En.of Bending');
 ylabel('Newtons*meters');
 box on
 axis([0 L+0.1*L -0.06 0.06]);
```

```
subplot(3,3,3);
plot(T,potential_energy_shearing); grid;
title('Potential En.of Shearing');
ylabel('Newtons*meters');
box on
axis([0 L+0.1*L -0.01 0.01]);

subplot(3,3,4);
plot(T,kinetic_energy_transv_deflec); grid;
title('      Kinetic En.of Transv.Defl.');
ylabel('Newtons*meters');
box on
axis([0 L+0.1*L -0.00000001 0.00000001]);

subplot(3,3,5);
plot(T,work_external_transv_load); grid;
title('Work by Ext.Transv.Load');
ylabel('Newtons*meters');
box on
axis([0 L+0.1*L -0.1 0.1]);

subplot(3,3,6);
plot(T,work_piezoelectric_control_force); grid;
title('Work by Piezoel. Force');
ylabel('Newtons*meters');
box on
axis([0 L+0.1*L -0.1 0.1]);

subplot(3,3,7);
plot(T,work_dissipated_viscoelastic_core); grid;
title('Work Dissipated in Viscoel.Core');
ylabel('Newtons*meters');
xlabel('Lengh  (meters)');
box on
axis([0 L+0.1*L -0.01 0.01]);

subplot(3,3,8);
plot(T,summary_energy); grid;
title('Total Energy');
ylabel('Newtons*meters');
box on
axis([0 L+0.1*L -0.015 0.015]);

subplot(3,3,9);
plot(T,transverse_displacement); grid;
title('Transv.Displ.of the Beam');
ylabel('W(x,t),  meters');
xlabel('Lengh  (meters)');
box on
axis([0 L+0.1*L -0.007 0.007]);

WL=z*a;
end;
```

APPENDIX D

ENERGIES

SIMULINK Block Diagram

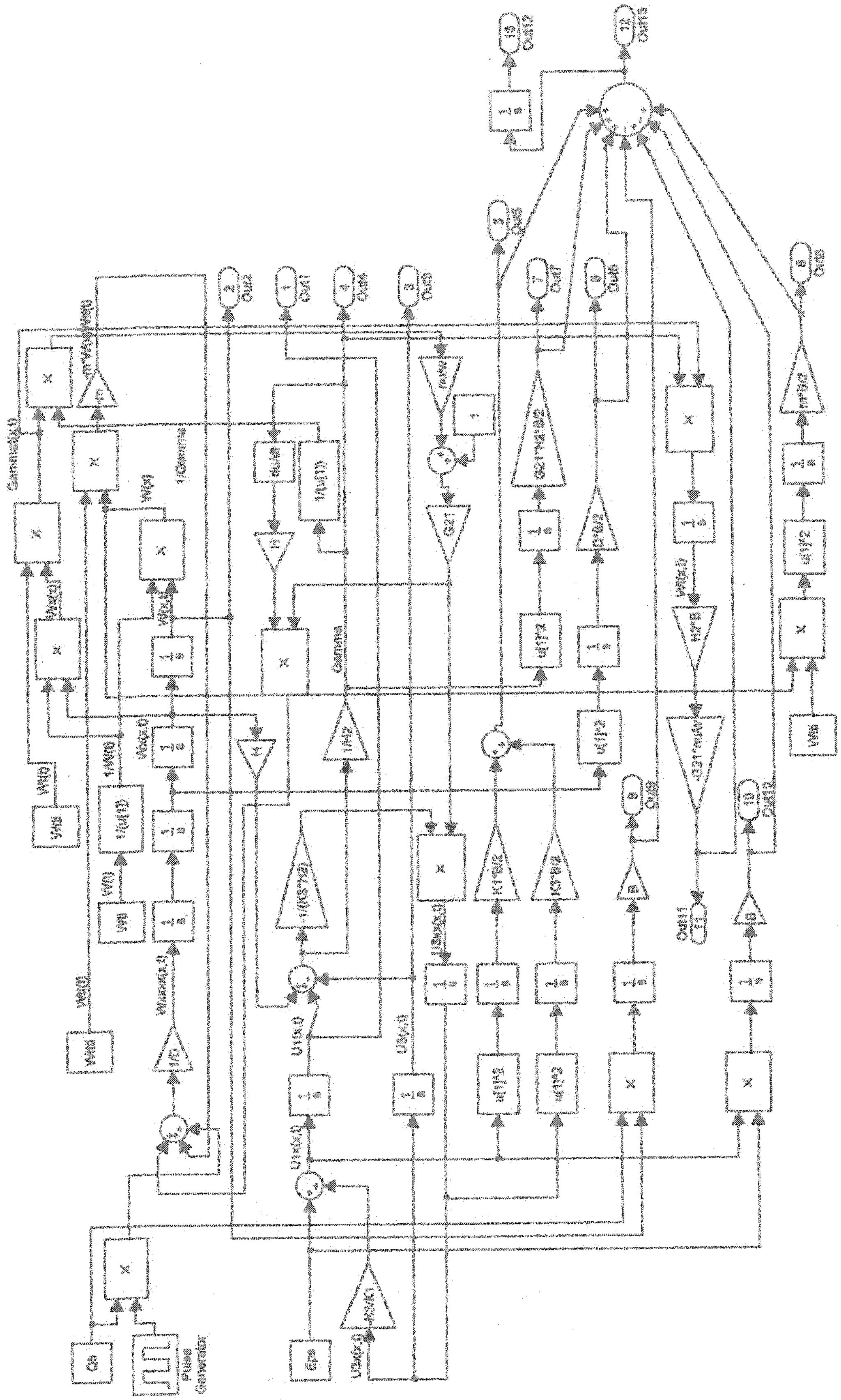

APPENDIX E

CONTROLLABILITY

MATLAB Program

APPENDIx E

```
   %Estimating of the Controllability with respect to the space distribution


%matrixes A and B for the state_space representation with respect to space
 i=sym('i');
 G21=sym('G21');
 nu=sym('nu');
 G2=G21*(1+nu*i);
 K1=sym('K1');
 K3=sym('K3');
 H=sym('H');
 H2=sym('H2');
 D=sym('D');
 m=sym('m');
 S=sym('S');

 B=[0;0;0;0;0;1/D];

A=[0                 1              0           0                  0              0;
   G2*(1/K1+1/K3)/H2 0              0           G2*H*(1/K1+1/K3)/H2 0             0;
   0                 0              0           1                  0              0;
   0                 0              0           0                  1              0;
   0                 0              0           0                  0              1;
  0                  G2*H/(D*H2)   -m*S*S/D    0                  G2*H*H/(D*H2)  0];

%det(A)
%ans =
%-G21*(1+i*nu)*(1/K1+1/K3)/H2*m*S^2/D



 AB=A*B;
 %maltiplicatiom of A and B (the second row of the controllability matrix M)
 %AB =[  0  0  0  0  1/D  0]

 A2=A*A;
 A2B=A2*B;
%maltiplication of A^2 and B (the 3-rd row of the controllability matrix M)
%A2B =
%[                     0]
%[                     0]
%[                     0]
%[                   1/D]
%[                     0]
%[ G21*(1+i*nu)*H^2/D^2/H2]

A3=A2*A;
A3B=A3*B;
%maltiplication of A^3 and B (the 4-th row of the controllability matrix M)
```

```
%A3B =
%[                                        0]
%[ G21*(1+i*nu)*H*(1/K1+1/K3)/H2/D]
%[                                      1/D]
%[                                        0]
%[           G21*(1+i*nu)*H^2/D^2/H2]
%[                                        0]

A4=A3*A;
A4B=A4*B;
%maltiplication of A^4 and B (the 5-th row of the controllability matrix M)
%A4B =
%[                                         G21*(1+i*nu)*H*(1/K1+1/K3)/H2/D]
%[                                                                       0]
%[                                                                       0]
%[                                                  G21*(1+i*nu)*H^2/D^2/H2]
%[                                                                       0]
%(G21^2*(1+i*nu)^2*H^2/D/H2^2*(1/K1+1/K3)-m*S^2/D+G21^2*(1+i*nu)^2*H^4/D^2/H2^2)/D]

A5=A4*A;
A5B=A5*B;
%maltiplication of A^5 and B (the 6-th row of the controllability matrix M)
%A5B =
%[                                                                          0]
%[ (G21^2*(1+i*nu)^2*(1/K1+1/K3)^2/H2^2*H+G21^2*(1+i*nu)^2*H^3*(1/K1+1/K3)/H2^2/D)/D]
%[                                                    G21*(1+i*nu)*H^2/D^2/H2]
%[                                                                          0]
%[ (G21^2*(1+i*nu)^2*H^2/D/H2^2*(1/K1+1/K3)-m*S^2/D+G21^2*(1+i*nu)^2*H^4/D^2/H2^2)/D]
%[                                                                          0]

%Formation of the controllability matrix M
M=[0    0    0                    0                                    G21 ...
*(1+i*nu)*H*(1/K1+1/K3)/H2/D                                            0;
0    0    0                    G21*(1+i*nu)*H*(1/K1+1/K3)/H2/D   0     ...
                                                              (G21^2*(1+i* ...
nu)^2*(1/K1+1/K3)^2/H2^2*H+G21^2*(1+i*nu)^2*H^3*(1/K1+1/K3)/H2^2/D)/D;
0    0    0                    1/D                                0     ...
                                                              G21*(1+i*nu) ...
*H^2/D^2/H2;
0    0    1/D                  0                                  G21*(1 ...
+i*nu)*H^2/D^2/H2                                             0;
0    1/D  0                    G21*(1+i*nu)*H^2/D^2/H2            0     ...
                                                              (G21^2*(1+i* ...
nu)^2*H^2/D/H2^2*(1/K1+1/K3)-m*S^2/D+G21^2*(1+i*nu)^2*H^4/D^2/H2^2)/D;
1/D  0    G21*(1+i*nu)*H^2/D^2/H2  0                              (G21^2 ...
*(1+i*nu)^2*H^2/D/H2^2*(1/K1+1/K3)-m*S^2/D+G21^2*(1+i*nu)^2*H^4/D^2/H2^2)/D   0   ...
                                                         ];
det(M)
%determinant of matrix M as the criteria of complete controllability
ans =
1/D^6*G21^3*(1+i*nu)^3*H^2*(K3+K1)^3/K1^3/K3^3/H2^3
```

APPENDIX F

STABILITY

MATLAB Program

```
G21=350000;          nu=1.5;
H1=0.000625;         H2=0.0025;          H3=0.00125;
H=H2+H1/2+H3/2;
E1=63000000;         E3=206850000;
K1=E1/H1;            K3=E3/H3;
L=0.1;               H4=0.05*L;          B=0.1*L;
I1=B*((2*H1+2*H2+2*H3+H4)^3-(2*H2+2*H3+H4)^3)/12;
I3=B*(2*H3+H4)^3/3;
D=(E1*I1+E3*I3)/B;                       m=0.05/(B*L);
WL=0.005;
QL=1000000;          n=1;
w=(n*pi/L)^2*sqrt(E1*I1+E3*I3/(m*(H1+H2+H3)*B));
wd=100;        f=wd/(2*pi);       Eps=0;

figure(1);    clf;
for ti = 2*pi:0.001:2.065*pi
     Qti=sin(wd*ti);
     Wti=QL*(wd*ti-sin(wd*ti))/(m*WL/wd^2);
     Wtti=QL*(1-cos(wd*ti))/(m*WL*wd);
     Wttti=QL*(sin(wd*ti))/(m*WL);
     [T,X,Y]=sim('Attachment7',[0,L]);
     displacement1=Y(:,1);
     transverse_displacement=Y(:,2);
     displacement3=Y(:,3);
     shear_strain_Gamma=Y(:,4);
     zmax=max(Y(:,2));
     zmin=min(Y(:,2));
     if abs(zmax)>abs(zmin)
         z=sign(zmax);
         a=abs(zmax);
    else z=sign(zmin);
         a=abs(zmin);
   end;
   Eps=-16*z*a;
x1=Y(:,5);
x2=Y(:,6);
x3=Y(:,2);
plot3(x1(end),x2(end),x3(end),'r.');
title('phase diagram');
zlabel('Wt(x,t),  meters/meters');
ylabel('Wx(x,t),  meters/seconds');
xlabel('W(x,t),  meters');
box on
axis([-0.15 0.15 -1 1 -0.01 0.01]);    %at 15-16
axis([-0.1 0.1 -2 2 -0.02 0.02]);    %at 0-5-16.5-17

WL=z*a;
hold on
end;
```

APPENDIX G

STABILITY

SIMULINK Block Diagram

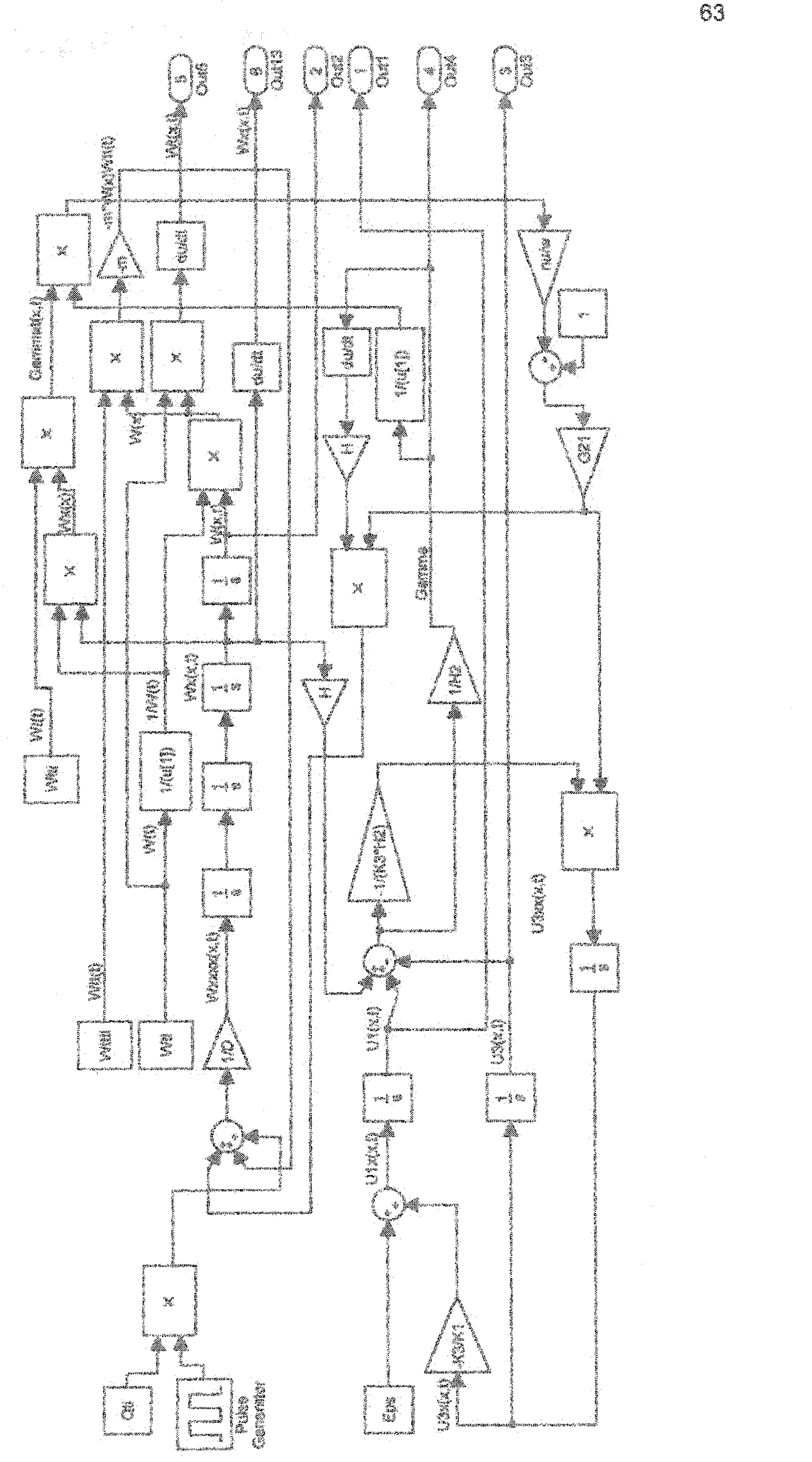

APPENDIX H

CONTROL DESIGN

MATLAB Program

OPTIMAL CONTROL DESIGN

APPENDIX H

```
G21=350000;             nu=1.5;
H1=0.000625;            H2=0.0025;           H3=0.00125;
H=H2+H1/2+H3/2;
E1=63000000;            E3=206850000;
K1=E1/H1;               K3=E3/H3;
L=0.1;                  H4=0.05*L;           B=0.1*L;
I1=B*((2*H1+2*H2+2*H3+H4)^3-(2*H2+2*H3+H4)^3)/12;
I3=B*(2*H3+H4)^3/3;
D=(E1*I1+E3*I3)/B;
m=0.1/(B*L);
WL=0.005;               QL=1000000;          n=1;
w=(n*pi/L)^2*sqrt(E1*I1+E3*I3/(m*(H1+H2+H3)*B));
wd=100;                 f=wd/(2*pi);         Eps=0;

figure(1); clf;
for ti = 2*pi:0.001:2.065*pi
    Qti=sin(wd*ti);
    Qtti=cos(ti);
    Wti=QL*(wd*ti-sin(wd*ti))/(m*WL/wd^2);
    Wtti=QL*(1-cos(wd*ti))/(m*WL*wd);
    Wttti=QL*(sin(wd*ti))/(m*WL);
    [T,X,Y]=sim('Attachment9',[0,L]);
    displacement1=Y(:,1);
    transverse_displacement=Y(:,2);
    displacement3=Y(:,3);
    shear_strain_Gamma=Y(:,4);
    potential_energy_extension=Y(:,5);
    potential_energy_bending=Y(:,6);
    potential_energy_shearing=Y(:,7);
    kinetic_energy_transv_deflec=Y(:,8);
    work_external_transv_load=Y(:,9);
    work_piezoelectric_control_force=Y(:,10);
    work_dissipated_viscoelastic_core=Y(:,11);
    zmax=max(Y(:,2));
    zmin=min(Y(:,2));
 if abs(zmax)>abs(zmin)
    z=sign(zmax);
    a=abs(zmax);
 else z=sign(zmin);
      a=abs(zmin);
  end;
  Eps_Optimal=z*Y(:,14);
  K=Eps Optimal/a;
```

```
subplot(2,2,1);
plot(T,displacement1); grid;
title('         Longitud.Defl.of Piezo-act');
ylabel('Displacement U1(x,t),meters');
xlabel('Lengh   (meters)');
box on
axis([0 L+0.1*L -0.000000001 0.000000003]);

 subplot(2,2,2);
 plot(T,transverse_displacement); grid;
 title('Transverse Displacement');
 ylabel('Displacement (meters)');
 xlabel('Lengh   (meters)');
 box on
 axis([0 L+0.1*L -0.01 0.01]);

  subplot(2,2,3);
  plot(T,Eps_Optimal); grid;
  title('  Control strain Eps');
  ylabel('Eps');
  xlabel('Lengh   (meters)');
  box on
  axis([0 L+0.1*L -0.1 0.1]);

  subplot(2,2,4);
  plot(T,K); grid;
  title('Control Gain Kg');
  ylabel('Control Gain (1/meters)');
  xlabel('Lengh   (meters)');
  box on
  axis([0 L+0.1*L -20 20]);

  WL=z*a;
  end;
  Kg=max(abs(Eps_Optimal))/a;
  Kg
  ;

%  Result

% Kg = 16.0465
```

APPENDIX I

CONTROL DESIGN

SIMULINK Block Diagram

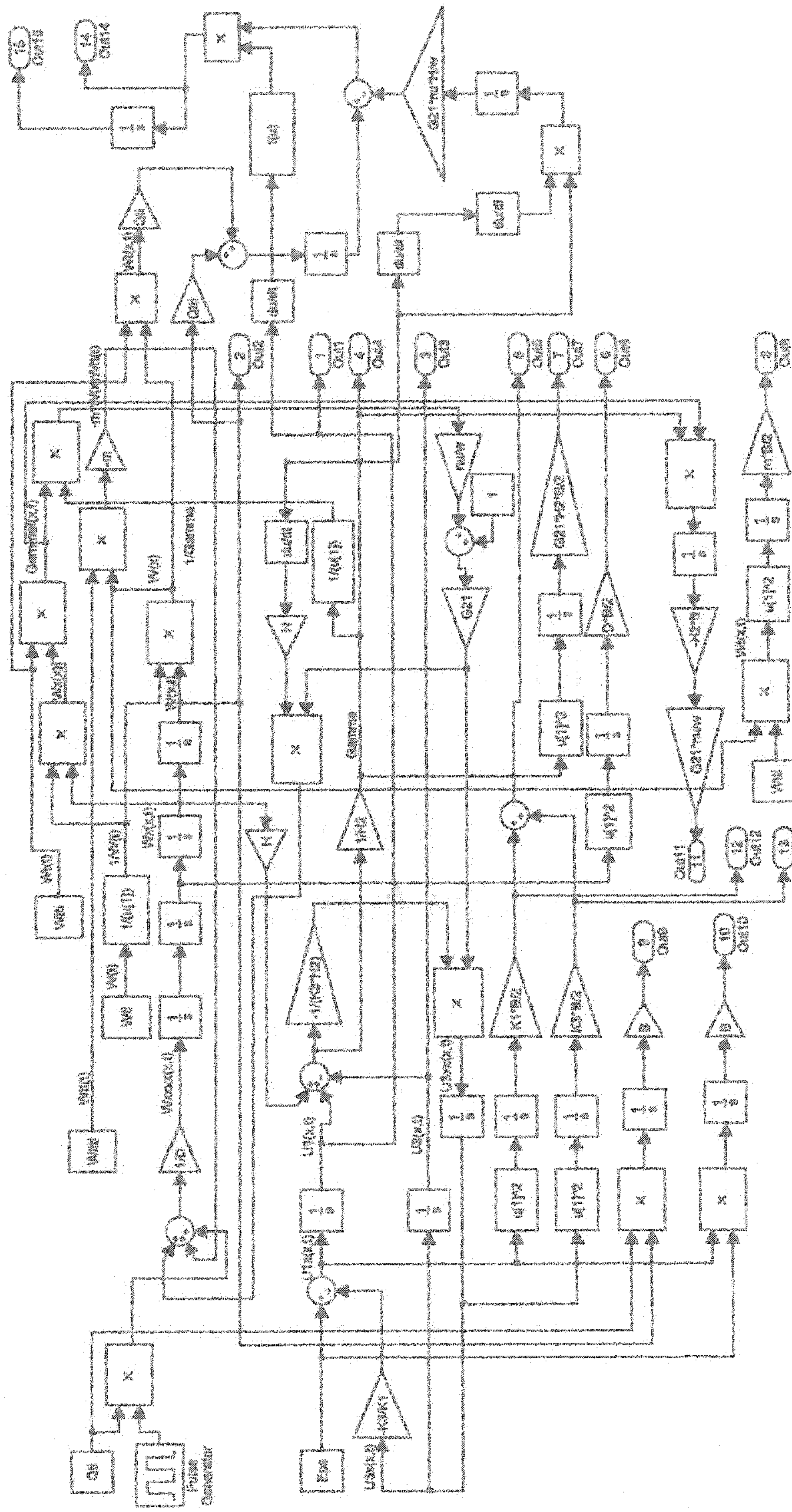

REFERENCES

1. Agafa, M., Baz, A., "Dynamics of Active Piezoelectric Damping composites", *Composites, Part B: engineering*, Vol. 31, pp.255-264, 2000.

2. Agnes, G.S., and Napolitano, K., "Active Constrained Layer Viscoelastic Damping", *in Proceedings of the 34th Structures, Structures Dynamics, and Material Conference*, 3499-3506, 1993.

3. Austin, E.A., "Variations on Modeling of Constrained-Layer Damping Treatments', *The Shock and Vibration Digest*, Vol. 31(4), pp.275-280, 1999.

4. Azvine, B., Tomlinson, G.R. and Wynne, R.J., "Use of Active Constrained-Layer Damping for Controlling Resonant Vibration", *Smart Materials and Structures*, Vol. 4, pp. 1-6, 1995.

5. Badre, A., Wang, K.W. and Gandhi, F., "An Analysis of Interlaminar Stresses in Active Constrained Layer Damping Treatments", *Journal of Sound and Vibration*, 2004.

6. Balamurugan, V., "Finite Element Formulation and Active Vibration Control Study on Beams Using Smart Constrained Layer Damping Treatment", *Journal of Sound and Vibration*, Vol. 249(2), pp. 227-250, 2002.

7. Balamurugan, V. and Narayanan S., " Active-Passive Hybrid Damping in Beams with Enhanced Smart Constrained Layer Treatment", *Engineering Structures*, Vol. 24, pp. 355-363, 2002.

8. Batra, R.C. and Yu, J.H., "Effect of Inertia Forces on the Damping of a Constrained Layer Finitely Deformed in Shearing, Letters to the Editor", *Journal of Sound and Vibration*, Vol. 241(5), pp. 913-919, 2001.

9. Baz, A., "Dynamic Boundary Control of Beams Using Active Constrained Layer Damping", *Mechanical Systems and Signal Processing*, Vol. 11(6), pp. 811-825, 1997.

10. Baz, A., "Robust Control of Active Constrained Layer Damping", *Journal of Sound and Vibration*, Vol. 211(3), pp. 467-480, 1998.

11. Baz, A. and Chen, T., "Control of Axi-Symmetric Vibrations of Cylindrical Shells Using Active Constrained Layer Damping", *Thin-Walled Structures*, Vol. 36, pp. 1-20, 2000.

12. Chen, Q. and Levy, C., "Vibration Analysis and Control of Flexible Beam by Using Smart Damping Structures", *Composites, Part B: engineering*, Vol. 30, pp. 395-406, 1999.

13. DiTaranto, R., "Static Analysis of a Laminated Beam", *ASME Journal of Engineering for Industry*, Vol. 95, pp.755-761, 1973.

14. Douglas, B. and Yang, J., "Transverse Compressional Damping in Vibratory Response of Elastic-Viscoelastic-Elastic Beams", *AIAA Journal*, Vol. 16, pp.925-930, 1978.

15. Hau, L. and Fung, E., "Effect of ACLD Treatment Configuration on Damping Performance of a Flexible Beam", *Journal of Sound and Vibration*, 2004.

16. Hibbeler, R.C., Mechanics of Materials, fifth edition, *Prentice Hall*, NJ, 2003.

17. Ingman, D.J., Engineering Vibrations, *Prentice Hall*, NJ, 2002.

18. Kreyszig, E., Advanced Engineering Mathematics, seventh edition, , *John Wiley & Sons Inc.*, New York, 1994.

19. Kung, S. W. and Singh, R., "Vibration Analysis of Beams with Multiple

Constrained Layer Damping Patches", *Journal of Sound and Vibration*, Vol. 212(5), pp. 781-805, 1998.

20. Kuo, B.C. and Golnaraghi, F., Automatic Control Systems, eight edition, *John Wiley & Sons Inc.*, New York, 2003.

21. Lee, U. and Kim, J., "Spectral Element Modelling for the Beams Treated with Active Constrained Layer Damping", *International Journal of Solids and Structures*, Vol. 38, pp. 5679-5702, 2001.

22. Levine, W.S., The Control, *Library of Congress Cataloging-in-Publication Data Handbook Published in Cooperation with IEEE Press*, 1996.

23. Levis, F.L and Syrmos, V.I., Optimal Control, second edition, *John Wiley & Sons Inc.*, New York, 2003.

24. Liao, W.H. and Wang, K.W., "On the Analysis of Viscoelastic Materials for Active constrained Layer Damping Treatments", *Journal of Sound and Vibration*, Vol. 207(3), pp. 319-334, 1997.

25. Liu, T.X., Hua, H.X. and Zhang, Z., "Robust Control of Plate Vibration via Active Constrained Layer Damping", *Thin-Walled Structures*, 2004.

26. Liu, Y., and Wang, K.W., "A Non-dimensional Parametric Study of Enhanced Active Constrained Layer Damping Treatments", *Journal of Sound and Vibration*, Vol. 223(4), pp. 611-644, 1999.

27. Liu, Y. and Wang, K.W., "Damping Optimization by Integrating Enhanced Active Constrained Layer and Active-Passive Hybrid constrained Layer Treatments", *Journal of Sound and Vibration*, Vol. 255(4), pp. 763-775, 2002.

28. Mead, D. and Markus, S., "The Forced Vibration of a Three-Layer Sandwiched

Beam with Arbitrary Boundary Conditions", *Journal of Sound and Vibration*, Vol. 10(1), pp. 163-175, 1969.

29. Meirovitch, L., Analytical Methods and Vibrations, New York: *MacMillan*, 1967.

30. Ogata, K., Modern Control Engineering, fourth edition, *Prentice Hall*, NJ, 2003.

31. Park, C.H. and Baz, A., " Vibration Control of Bending Modes of Plates Using Active Constrained Layer Damping", *Journal of Sound and Vibration*, Vol. 227(4), pp. 711-734, 1999.

32. Park, C.H. and Baz, A., "Comparison between Finite Element Formulation of Active Constrained Layer Damping Using Classical and Layer-wise Laminate theory", *Finite Elements in Analysis and Design*, Vol. 37, pp. 35-56, 2001.

33. Rao, S.S. and Sunar, M., "Pezoelectricity and its Use in Disturbance Sensing and Control of Flexible Structures: A Survey", *Applied Mechanical Review*, Vol. 47(4), pp. 113-123, 1994.

34. Ray, M.C. and Baz, A., "Optimization of Energy Dissipation of Active Constrained Layer damping Treatments of Plates", *Journal of Sound and Vibration*, Vol. 208(3), pp. 391-406, 1997.

35. Ray, M.C., Oh, J. and Baz A., "Active Constrained Layer Damping of thin Cylindrical Shells", *Journal of Sound and Vibration*, Vol. 240(5), pp. 921-935, 2001.

36. Ro, J. and Baz, A., "Optimum Placement and Control of Active Constrained Layer Damping", *in Proceedings of the SPIE*, Vol. 3329, pp.844-855, 1998.

37. Ruzzene, M., Oh, J. and Baz, A., "Finite Element Modelling of Magnetic Constrained Layer Damping", *Journal of Sound and Vibration*, Vol. 236(4), pp. 657-682, 2000.

38. Serway, R.A. and Beichner, R.J., Physics for Scientists and Engineers with Modern Physics, fifth edition, *Thomson Learning Inc.*, 2003.

39. Shen, I.Y., "Intelligent Constrained Layer: An Innovative approach", *ASME Intelligent Structures, Materials and Vibration*, Vol. DE-58, pp.75-82, 1993.

40. Silva, C.W. Vibration, Fundamentals and Practice, *Library of Congress Cataloging-in-Publication Data*, 2000.

41. Sun, D. and Tong, L., "Modelling and Vibration Control of Beams with Partially Debonded Active Constrained Layer Damping Patch", *Journal of Sound and Vibration*, Vol. 252(3), pp. 493-507, 2002.

42. Trindade, M.A., Benjeddou, A. and Ohayon, R., "Finite Element Modelling of Hybrid Active-Passive Vibration Damping of Multilayer Piezoelectric Sandwich Beams – Part II: System Analysis", *International Journal for Numerical Methods in Engineering*, Vol. 51, pp. 855-864, 2001.

43. Vincent, T.L. and Grantham, W.J., Nonlinear and Optimal Control Systems, *John Wiley & Sons Inc.*, New York, 2003.

44. Van Nostrand, W.C. and Inman, D.J., "Finite Element Model for Active Constrained Layer Damping", *in SPIE North American Conference on Smart Structures and Materials*, Vol.2427, pp.124-139, 1995.

45. Yu, J.H. and Batra, R.C., "Constrained Layer Damping in Finite Shearing Deformations", *Journal of Sound and Vibration*, Vol. 229(2), pp. 445-452, 2000.

VITA

EDUCATION:

Master of Science in Mechanical Engineering, from University of Texas Pan-American, expected graduation date: May, 2004; cumulative GPA-3.95/4.00 .

Master of Business Administration, from University of Texas Pan-American, expected graduation date: August, 2005; cumulative current GPA-4.00/4.00 .

Post - graduated in Geophysics, completed, from Marine Hydro-Physics Institute of National Academy of Sciences of Ukraine, 1996.

Master of Science in Applied Mathematics, Moscow State University, Engineering - Physics Institute, 1989.

Bachelor of Science in Industrial Engineering, Moscow State University, Engineering - Physics Institute, 1987.

EXPERIENCE:

1989-1993: Engineer - Designer, Design - Construction Department of Central Technological Assembly of Ukraine.

1993-1996: Post-graduate Aspirant, Marine Hydro - Physics Institute of National Academy of Science of Ukraine.

1995-1999: Instructor of Mathematics at Sevastopol Technical College, Ukraine.

1994-2001: Engineer - Mathematician, Marine Hydro-Physics Institute of National Academy of Science of Ukraine; application of mathematical methods of engineering physics for research tasks.

2002-2003: Research - Assistant, University of Texas Pan -American, Engineering Department; responsible for mechanical testing, and automatic control tuning to make the investigated system reliable with no impact to station operations.

2002-present: Project Engineer-Manager, Hiway Neon Signs Co., Pharr, Texas; decision making authority for design, development, manufacturing of electrical, neon signs and electronic digital boards, provide support to client operations.

ORGANIZATIONS:

American Society of Mechanical Engineers, American Society of Women Engineers.

CERTIFICATES:

Certificate СПК #61458 of Instructor of Mathematics at Educational Institutions, 1998.

Certificate # 78/1009-38, Completed Post-Graduate Education in Geophysics, 1996.

Diploma НВ #580446 of Master's Degree in Applied Mathematics, 1989.

Diploma НВ #580446 of Bachelor's Degree in Industrial Engineering, 1987.

PUBLICATIONS:

Generation of Long Barotropic Waves by Moving Disturbance of Pressure in Systems of Basins Connected by Strait./ A.V.Konovalov, T.G.Korokova, L.V.Cherkesov// *Thermo-Hydrodynamics of Ocean, Marine Hydro-Physics Journal*, 1998, 1, pp.3-15.

PERSONAL PROFILE:

Born on March, 18, 1966 in Cheboksary, Russia; lived in Sevastopol city, Ukraine; currently Permanent Resident of United States.